PCNA is released and left behind, and RFC incorporates PCNA that slides back to the 3′-end or reloads PCNA from solution.[33] These are dynamic and stochastic events. When PCNA molecules accumulate on DNA, the probability of reutilization is much higher than that of reloading from solution.[33] Thus, at growing ends, ubiquitin-free PCNA molecules normally tend to be loaded from solution. Under these circumstances, ubiquitinated PCNA molecules are not retained proximately to the 3′-ends so that pol η is restricted from association. At a stalled 3′-end, PCNA molecules are quickly accumulated onto DNA until reaching saturation. Consequently, the same PCNA molecule stays proximately to the stalled 3′-end. Once the PCNA molecule is ubiquitinated, it persists until pol η associates through interaction with the mono-ubiquitinated PCNA and extends the 3′-end. Once DNA synthesis is restored, PCNA molecules on DNA are diluted, facilitating reloading of fresh PCNA from solution and reducing the probability of pol η access.

Importantly, our results in the human system are quite different from some recent reports with a yeast system,[57,58] but not all.[48,55] In those reports,[57,58] it seems that pol δ is stably associated with PCNA during elongation but destabilizes with stalling replication. Such destabilization is more significant when PCNA is mono-ubiquitinated. Once pol η binds to ubiquitinated PCNA, association of pol δ is prohibited. Therefore, it is possible that some factors, which can stabilize pol δ–PCNA and pol η–PCNA interactions, could be missing in this human *in vitro* system.[33,37,38,54] Our system could thus be useful to address such missing factors for further understanding of molecular mechanisms of polymerase switching in humans.

Materials and Methods

Proteins

Recombinant human proteins were overproduced in *E. coli* cells and purified by conventional column chromatography. Detailed procedures for plasmid construction and protein purification are described in the Supplementary Data.

PCNA mono-ubiquitination assays

The standard reaction mixture (25 μl) contained 20 mM Hepes–NaOH (pH 7.5); 50 mM NaCl; 0.2 mg/ml bovine serum albumin (BSA); 1 mM DTT; 10 mM $MgCl_2$; 1 mM ATP; 0.1 mM each of dGTP, dATP, dCTP, and dTTP; 33 fmol of singly primed mp18 ssDNA (with the 90-mer primer, CTGCAAGGCGATTAAGTTGGGTAACGCCAGGGTTTTCCCAGTCACGACGTTGTAAAACGACGGCCAGTGCCAAGCTTGCATGCCTGCAGG); RPA (9 pmol); PCNA (1 pmol); RFC (88 fmol); E1 (850 fmol); RAD6A–RAD18 complex (950 fmol); and ubiquitin (170 pmol). Reaction mixtures were prepared on ice and then incubated at 30 °C for the indicated times. After termination of reactions with addition of 2 μl of 300 mM ethylenediaminetetraacetic acid (EDTA), the mixtures were immediately chilled on ice. Ubiquitination of PCNA was measured by Western analysis with an anti-PCNA antibody (Santa Cruz, sc-7907). Detection was carried out using an ECL chemiluminescence kit (GE Healthcare, Tokyo, Japan) and a CCD camera.

For ubiquitination assays with poly(dA)–oligo(dT), 100 ng of DNA including 900 fmol of oligo(dT) (GE Healthcare), instead of 33 fmol of mp18 DNA, was mixed under the standard reaction conditions except for the omission of dNTPs, RPA and RFC.

DNA replication assays

The standard reaction mixtures with [α-^{32}P]dTTP (25 μl) were preincubated at 30 °C for 1 min, and then reactions were started by addition of pol δ (380 fmol). After incubation at 30 °C for the indicated times, reactions were terminated with 2 μl of 300 mM EDTA, and the mixtures were immediately chilled on ice. Products of DNA synthesis were analyzed as described earlier.[33] Gel images of autoradiography were analyzed by Multi Gauge software Version 3.0 (FUJIFILM, Tokyo, Japan).

For replication assays with poly(dA)–oligo(dT), 100 ng of DNA including 900 fmol of oligo(dT) (GE Healthcare), instead of 33 fmol of mp18 DNA, was mixed under the standard reaction conditions including [α-^{32}P]dTTP, but not other dNTPs, RPA and RFC.

PCNA mono-ubiquitination of DNA–PCNA complexes isolated by gel filtration

For the introduction of nicks, plasmid pUC18 was reacted with N.BstNBI (New England BioLabs, Tokyo, Japan) at 55 °C for 60 min. Then, DNA was extracted with phenol/chloroform and precipitated with ethanol. PCNA (8 pmol), RFC$^{(p140N555)}$ (36 fmol), and the nicked plasmid pUC18 (133 fmol) were incubated at 30 °C for 15 min in 100 μl of buffer containing 20 mM Hepes–NaOH (pH 7.5), 100 mM NaCl, 0.2 mg/ml BSA, 1 mM DTT, 10 mM $MgCl_2$, and 1 mM ATP. The mixture was then immediately applied at room temperature to a 2-ml column of 4% agarose beads (A-1040-S, Agarose Beads Technologies, Madrid, Spain) equilibrated in buffer containing 20 mM Hepes–NaOH (pH 7.5), 1 mM DTT, 10 mM $MgCl_2$, and 50 mM NaCl, and fractions of three drops each were collected on ice. The fractions eluted in void volume containing DNA were pooled, and then 12.5-μl aliquots were incubated with E1 (850 fmol), RAD6A–RAD18 complex (38 fmol), and ubiquitin (170 pmol) in the presence of the indicated amounts of RFC or pol δ at 30 °C for 30 min in 25-μl reaction mixtures [20 mM Hepes–NaOH (pH 7.5), 50 mM NaCl, 0.2 mg/ml BSA, 1 mM DTT, 10 mM $MgCl_2$, 1 mM ATP, and 0.1 mM each of dGTP, dATP, and dTTP].

Isolation of PCNA on DNA bound to magnetic beads

The 5′-biotinylated primer (TCTCTCTCTCTGCAAGGCGATTAAGTTGGGTAACGCCAGGGTTTTCCCAGTCACGACGTTGTAAAACGACGGCCAGTGCCAAGCTTGCATGCCTGCAGG) was annealed to 33 fmol mp18 ssDNA and immobilized onto a 10-μl suspension of streptavidin magnetic beads, Dynabeads M280 (Life Technologies, Tokyo, Japan), as described previously.[33] Assays were carried out under standard reaction conditions as described for Fig. 4c. After termination of the reactions with 2 μl of 300 mM EDTA, the beads were washed and analyzed.[33]

Assay for PCNA mono-ubiquitination-dependent polymerase switching

RPA (900 fmol), PCNA (1 pmol), RFC (26 fmol), E1 (850 fmol), RAD6A–RAD18 complex (950 fmol), ubiquitin (170 pmol), and 3.3 fmol of singly primed mp18 ssDNA (with the 36-mer primer, CAGGGTTTTCCCAGTCACGACGTTGTAAAACGACGG) were mixed under standard reaction conditions with [α-^{32}P]dTTP in the presence or absence of pol η (10 fmol). After incubation at 30 °C for 1 min, pol δ (750 fmol) was added and the mixture was further incubated for the indicated times. Reaction products (10 μl) were analyzed by 0.7% alkaline agarose gel electrophoresis.[33] Gel images of autoradiography were analyzed by Multi Gauge software Version 3.0 (FUJIFILM).

Acknowledgements

We thank Dr. Marc S. Wold (University of Iowa College of Medicine, Iowa City, IA), Dr. Fumio Hanaoka (Osaka University, Osaka, Japan), Dr. Toshiki Tsurimoto (Kyushu University, Fukuoka, Japan), Dr. Tomohiko Ohta (St. Marianna University School of Medicine, Kanagawa, Japan), and Dr. Tadashi Shimamoto (Hiroshima University, Hiroshima, Japan) for respectively providing an RPA expression plasmid, *POLH* cDNA, a PCNA expression plasmid, a ubiquitin-encoding plasmid, and an *E. coli* strain to produce mp18 ssDNA. Several cloning vectors were obtained from the National BioResource Project (National Institute of Genetics, Japan). We also thank Dr. Niels de Wind (Leiden University Medical Center, Leiden, The Netherlands) and Dr. Hiroshi Hashimoto (Yokohama City University, Kanagawa) for their comments and suggestions on the manuscript. We are grateful to Kenji Masuda for his help with cDNA cloning and Tomoka Nakashima, Fumie Okubo, Kazumi Shimamoto, Miki Suzuki, and Mai Yoshida for their laboratory assistance. This work was supported by Grants-in-Aid from the Ministry of Education, Culture, Sports, Science and Technology of Japan (to Y.M. and K.K.); by the 21st Century Center of Excellence program from the Ministry of Education, Culture, Sports, Science and Technology of Japan (to K.K.); by Health and Labour Science Research Grants (to K.K.); by Grants-in-Aid for Cancer Research from the Ministry of Health, Labour and Welfare (to K.K.); and by the Radiation Effects Association (to Y.M.). During the performance of this work, J.P. was supported by a Japan Society for the Promotion of Science Research Fellowship for Young Scientists.

Supplementary Data

Supplementary data associated with this article can be found, in the online version, at doi:10.1016/j.jmb.2010.01.003

References

1. Hishida, T., Kubota, Y., Carr, A. M. & Iwasaki, H. (2009). *RAD6–RAD18–RAD5*-pathway-dependent tolerance to chronic low-dose ultraviolet light. *Nature*, **457**, 612–615.
2. Lehmann, A. R., Niimi, A., Ogi, T., Brown, S., Sabbioneda, S., Wing, J. F. *et al.* (2007). Translesion synthesis: Y-family polymerases and the polymerase switch. *DNA Repair (Amst.)*, **6**, 891–899.
3. Andersen, P. L., Xu, F. & Xiao, W. (2008). Eukaryotic DNA damage tolerance and translesion synthesis through covalent modifications of PCNA. *Cell Res.* **18**, 162–173.
4. Hoege, C., Pfander, B., Moldovan, G. L., Pyrowolakis, G. & Jentsch, S. (2002). RAD6-dependent DNA repair is linked to modification of PCNA by ubiquitin and SUMO. *Nature*, **419**, 135–141.
5. Stelter, P. & Ulrich, H. D. (2003). Control of spontaneous and damage-induced mutagenesis by SUMO and ubiquitin conjugation. *Nature*, **425**, 188–191.
6. Watanabe, K., Tateishi, S., Kawasuji, M., Tsurimoto, T., Inoue, H. & Yamaizumi, M. (2004). Rad18 guides polη to replication stalling sites through physical interaction and PCNA monoubiquitination. *EMBO J.* **23**, 3886–3896.
7. Bailly, V., Lamb, J., Sung, P., Prakash, S. & Prakash, L. (1994). Specific complex formation between yeast RAD6 and RAD18 proteins: a potential mechanism for targeting RAD6 ubiquitin-conjugating activity to DNA damage sites. *Genes Dev.* **8**, 811–820.
8. Bailly, V., Lauder, S., Prakash, S. & Prakash, L. (1997). Yeast DNA repair proteins Rad6 and Rad18 form a heterodimer that has ubiquitin conjugating, DNA binding, and ATP hydrolytic activities. *J. Biol. Chem.* **272**, 23360–23365.
9. Garg, P. & Burgers, P. M. (2005). Ubiquitinated proliferating cell nuclear antigen activates translesion DNA polymerases η and REV1. *Proc. Natl Acad. Sci. USA*, **102**, 18361–18366.
10. Haracska, L., Unk, I., Prakash, L. & Prakash, S. (2006). Ubiquitylation of yeast proliferating cell nuclear antigen and its implications for translesion DNA synthesis. *Proc. Natl Acad. Sci. USA*, **103**, 6477–6482.
11. Xin, H., Lin, W., Sumanasekera, W., Zhang, Y., Wu, X. & Wang, Z. (2000). The human *RAD18* gene product interacts with HHR6A and HHR6B. *Nucleic Acids Res.* **28**, 2847–2854.
12. Yuasa, M. S., Masutani, C., Hirano, A., Cohn, M. A., Yamaizumi, M., Nakatani, Y. & Hanaoka, F. (2006). A human DNA polymerase η complex containing Rad18, Rad6 and Rev1; proteomic analysis and targeting of the complex to the chromatin-bound fraction of cells undergoing replication fork arrest. *Genes Cells*, **11**, 731–744.
13. Unk, I., Hajdu, I., Fatyol, K., Szakal, B., Blastyak, A., Bermudez, V. *et al.* (2006). Human SHPRH is a ubiquitin ligase for Mms2-Ubc13-dependent polyubiquitylation of proliferating cell nuclear antigen. *Proc. Natl Acad. Sci. USA*, **103**, 18107–18112.
14. Bi, X., Barkley, L. R., Slater, D. M., Tateishi, S., Yamaizumi, M., Ohmori, H. & Vaziri, C. (2006). Rad18 regulates DNA polymerase κ and is required for recovery from S-phase checkpoint-mediated arrest. *Mol. Cell. Biol.* **26**, 3527–3540.
15. Bienko, M., Green, C. M., Crosetto, N., Rudolf, F., Zapart, G., Coull, B. *et al.* (2005). Ubiquitin-binding domains in Y-family polymerases regulate translesion synthesis. *Science*, **310**, 1821–1824.

16. Guo, C., Tang, T. S., Bienko, M., Parker, J. L., Bielen, A. B., Sonoda, E. *et al.* (2006). Ubiquitin-binding motifs in REV1 protein are required for its role in the tolerance of DNA damage. *Mol. Cell. Biol.* **26**, 8892–8900.
17. Kannouche, P. L., Wing, J. & Lehmann, A. R. (2004). Interaction of human DNA polymerase η with monoubiquitinated PCNA: a possible mechanism for the polymerase switch in response to DNA damage. *Mol. Cell*, **14**, 491–500.
18. Plosky, B. S., Vidal, A. E., Fernandez de Henestrosa, A. R., McLenigan, M. P., McDonald, J. P., Mead, S. & Woodgate, R. (2006). Controlling the subcellular localization of DNA polymerases ι and η via interactions with ubiquitin. *EMBO J.* **25**, 2847–2855.
19. Motegi, A., Sood, R., Moinova, H., Markowitz, S. D., Liu, P. P. & Myung, K. (2006). Human SHPRH suppresses genomic instability through proliferating cell nuclear antigen polyubiquitination. *J. Cell Biol.* **175**, 703–708.
20. Motegi, A., Liaw, H. J., Lee, K. Y., Roest, H. P., Maas, A., Wu, X. *et al.* (2008). Polyubiquitination of proliferating cell nuclear antigen by HLTF and SHPRH prevents genomic instability from stalled replication forks. *Proc. Natl Acad. Sci. USA*, **105**, 12411–12416.
21. Unk, I., Hajdu, I., Fatyol, K., Hurwitz, J., Yoon, J. H., Prakash, L. *et al.* (2008). Human HLTF functions as a ubiquitin ligase for proliferating cell nuclear antigen polyubiquitination. *Proc. Natl Acad. Sci. USA*, **105**, 3768–3773.
22. Arakawa, H., Moldovan, G. L., Saribasak, H., Saribasak, N. N., Jentsch, S. & Buerstedde, J. M. (2006). A role for PCNA ubiquitination in immunoglobulin hypermutation. *PLoS Biol.* **4**, e366.
23. Edmunds, C. E., Simpson, L. J. & Sale, J. E. (2008). PCNA ubiquitination and REV1 define temporally distinct mechanisms for controlling translesion synthesis in the avian cell line DT40. *Mol. Cell*, **30**, 519–529.
24. Langerak, P., Nygren, A. O., Krijger, P. H., van den Berk, P. C. & Jacobs, H. (2007). A/T mutagenesis in hypermutated immunoglobulin genes strongly depends on $PCNA^{K164}$ modification. *J. Exp. Med.* **204**, 1989–1998.
25. Delbos, F., De Smet, A., Faili, A., Aoufouchi, S., Weill, J. C. & Reynaud, C. A. (2005). Contribution of DNA polymerase η to immunoglobulin gene hypermutation in the mouse. *J. Exp. Med.* **201**, 1191–1196.
26. Martomo, S. A., Yang, W. W., Wersto, R. P., Ohkumo, T., Kondo, Y., Yokoi, M. *et al.* (2005). Different mutation signatures in DNA polymerase η- and MSH6-deficient mice suggest separate roles in antibody diversification. *Proc. Natl Acad. Sci. USA*, **102**, 8656–8661.
27. Zeng, X., Winter, D. B., Kasmer, C., Kraemer, K. H., Lehmann, A. R. & Gearhart, P. J. (2001). DNA polymerase η is an A–T mutator in somatic hypermutation of immunoglobulin variable genes. *Nat. Immunol.* **2**, 537–541.
28. Frampton, J., Irmisch, A., Green, C. M., Neiss, A., Trickey, M., Ulrich, H. D. *et al.* (2006). Postreplication repair and PCNA modification in *Schizosaccharomyces pombe*. *Mol. Biol. Cell*, **17**, 2976–2985.
29. Simpson, L. J., Ross, A. L., Szuts, D., Alviani, C. A., Oestergaard, V. H., Patel, K. J. & Sale, J. E. (2006). RAD18-independent ubiquitination of proliferating-cell nuclear antigen in the avian cell line DT40. *EMBO Rep.* **7**, 927–932.
30. Huang, T. T., Nijman, S. M., Mirchandani, K. D., Galardy, P. J., Cohn, M. A., Haas, W. *et al.* (2006). Regulation of monoubiquitinated PCNA by DUB autocleavage. *Nat. Cell Biol.* **8**, 339–347.
31. Oestergaard, V. H., Langevin, F., Kuiken, H. J., Pace, P., Niedzwiedz, W., Simpson, L. J. *et al.* (2007). Deubiquitination of FANCD2 is required for DNA crosslink repair. *Mol. Cell*, **28**, 798–809.
32. Davies, A. A., Huttner, D., Daigaku, Y., Chen, S. & Ulrich, H. D. (2008). Activation of ubiquitin-dependent DNA damage bypass is mediated by replication protein A. *Mol. Cell*, **29**, 625–636.
33. Masuda, Y., Suzuki, M., Piao, J., Gu, Y., Tsurimoto, T. & Kamiya, K. (2007). Dynamics of human replication factors in the elongation phase of DNA replication. *Nucleic Acids Res.* **35**, 6904–6916.
34. Zuo, S., Bermudez, V., Zhang, G., Kelman, Z. & Hurwitz, J. (2000). Structure and activity associated with multiple forms of *Schizosaccharomyces pombe* DNA polymerase δ. *J. Biol. Chem.* **275**, 5153–5162.
35. Burgers, P. M. & Gerik, K. J. (1998). Structure and processivity of two forms of *Saccharomyces cerevisiae* DNA polymerase δ. *J. Biol. Chem.* **273**, 19756–19762.
36. Lee, M. Y., Tan, C. K., Downey, K. M. & So, A. G. (1984). Further studies on calf thymus DNA polymerase δ purified to homogeneity by a new procedure. *Biochemistry*, **23**, 1906–1913.
37. Podust, L. M., Podust, V. N., Sogo, J. M. & Hübscher, U. (1995). Mammalian DNA polymerase auxiliary proteins: analysis of replication factor C-catalyzed proliferating cell nuclear antigen loading onto circular double-stranded DNA. *Mol. Cell. Biol.* **15**, 3072–3081.
38. Podust, V. N., Chang, L. S., Ott, R., Dianov, G. L. & Fanning, E. (2002). Reconstitution of human DNA polymerase δ using recombinant baculoviruses: the p12 subunit potentiates DNA polymerizing activity of the four-subunit enzyme. *J. Biol. Chem.* **277**, 3894–3901.
39. Tsurimoto, T. & Stillman, B. (1991). Replication factors required for SV40 DNA replication *in vitro*. I. DNA structure-specific recognition of a primer-template junction by eukaryotic DNA polymerases and their accessory proteins. *J. Biol. Chem.* **266**, 1950–1960.
40. Fukuda, K., Morioka, H., Imajou, S., Ikeda, S., Ohtsuka, E. & Tsurimoto, T. (1995). Structure–function relationship of the eukaryotic DNA replication factor, proliferating cell nuclear antigen. *J. Biol. Chem.* **270**, 22527–22534.
41. Tsurimoto, T., Shinozaki, A., Yano, M., Seki, M. & Enomoto, T. (2005). Human Werner helicase interacting protein 1 (WRNIP1) functions as a novel modulator for DNA polymerase δ. *Genes Cells*, **10**, 13–22.
42. Shikata, K., Ohta, S., Yamada, K., Obuse, C., Yoshikawa, H. & Tsurimoto, T. (2001). The human homologue of fission Yeast cdc27, p66, is a component of active human DNA polymerase δ. *J. Biochem.* **129**, 699–708.
43. Burgers, P. M. & Yoder, B. L. (1993). ATP-independent loading of the proliferating cell nuclear antigen requires DNA ends. *J. Biol. Chem.* **268**, 19923–19926.
44. Uhlmann, F., Cai, J., Gibbs, E., O'Donnell, M. & Hurwitz, J. (1997). Deletion analysis of the large subunit p140 in human replication factor C reveals regions required for complex formation and replication activities. *J. Biol. Chem.* **272**, 10058–10064.
45. Podust, V. N., Tiwari, N., Stephan, S. & Fanning, E. (1998). Replication factor C disengages from proliferating cell nuclear antigen (PCNA) upon sliding clamp formation, and PCNA itself tethers DNA polymerase δ to DNA. *J. Biol. Chem.* **273**, 31992–31999.

46. Yao, N., Turner, J., Kelman, Z., Stukenberg, P. T., Dean, F., Shechter, D. *et al.* (1996). Clamp loading, unloading and intrinsic stability of the PCNA, β and gp45 sliding clamps of human, *E. coli* and T4 replicases. *Genes Cells*, **1**, 101–113.
47. Yuzhakov, A., Kelman, Z., Hurwitz, J. & O'Donnell, M. (1999). Multiple competition reactions for RPA order the assembly of the DNA polymerase δ holoenzyme. *EMBO J.* **18**, 6189–6199.
48. Chilkova, O., Stenlund, P., Isoz, I., Stith, C. M., Grabowski, P., Lundstrom, E. B. *et al.* (2007). The eukaryotic leading and lagging strand DNA polymerases are loaded onto primer-ends via separate mechanisms but have comparable processivity in the presence of PCNA. *Nucleic Acids Res.* **35**, 6588–6597.
49. Masutani, C., Kusumoto, R., Yamada, A., Dohmae, N., Yokoi, M., Yuasa, M. *et al.* (1999). The *XPV* (xeroderma pigmentosum variant) gene encodes human DNA polymerase η. *Nature*, **399**, 700–704.
50. Masutani, C., Araki, M., Yamada, A., Kusumoto, R., Nogimori, T., Maekawa, T. *et al.* (1999). Xeroderma pigmentosum variant (XP-V) correcting protein from HeLa cells has a thymine dimer bypass DNA polymerase activity. *EMBO J.* **18**, 3491–3501.
51. Haracska, L., Johnson, R. E., Unk, I., Phillips, B., Hurwitz, J., Prakash, L. & Prakash, S. (2001). Physical and functional interactions of human DNA polymerase η with PCNA. *Mol. Cell. Biol.* **21**, 7199–7206.
52. Haracska, L., Kondratick, C. M., Unk, I., Prakash, S. & Prakash, L. (2001). Interaction with PCNA is essential for yeast DNA polymerase η function. *Mol. Cell*, **8**, 407–415.
53. Kusumoto, R., Masutani, C., Shimmyo, S., Iwai, S. & Hanaoka, F. (2004). DNA binding properties of human DNA polymerase η: implications for fidelity and polymerase switching of translesion synthesis. *Genes Cells*, **9**, 1139–1150.
54. Tsurimoto, T. & Stillman, B. (1989). Multiple replication factors augment DNA synthesis by the two eukaryotic DNA polymerases, α and δ. *EMBO J.* **8**, 3883–3889.
55. McCulloch, S. D., Kokoska, R. J., Garg, P., Burgers, P. M. & Kunkel, T. A. (2009). The efficiency and fidelity of 8-oxo-guanine bypass by DNA polymerases δ and η. *Nucleic Acids Res.* **37**, 2830–2840.
56. Einolf, H. J. & Guengerich, F. P. (2000). Kinetic analysis of nucleotide incorporation by mammalian DNA polymerase δ. *J. Biol. Chem.* **275**, 16316–16322.
57. Langston, L. D. & O'Donnell, M. (2008). DNA polymerase δ is highly processive with proliferating cell nuclear antigen and undergoes collision release upon completing DNA. *J. Biol. Chem.* **283**, 29522–29531.
58. Zhuang, Z., Johnson, R. E., Haracska, L., Prakash, L., Prakash, S. & Benkovic, S. J. (2008). Regulation of polymerase exchange between Polη and Polδ by monoubiquitination of PCNA and the movement of DNA polymerase holoenzyme. *Proc. Natl Acad. Sci. USA*, **105**, 5361–5366.
59. Gulbis, J. M., Kelman, Z., Hurwitz, J., O'Donnell, M. & Kuriyan, J. (1996). Structure of the C-terminal region of p21(WAF1/CIP1) complexed with human PCNA. *Cell*, **87**, 297–306.
60. Jonsson, Z. O., Hindges, R. & Hübscher, U. (1998). Regulation of DNA replication and repair proteins through interaction with the front side of proliferating cell nuclear antigen. *EMBO J.* **17**, 2412–2425.
61. Georgescu, R. E., Kim, S. S., Yurieva, O., Kuriyan, J., Kong, X. P. & O'Donnell, M. (2008). Structure of a sliding clamp on DNA. *Cell*, **132**, 43–54.
62. Schmutz, V., Wagner, J., Janel-Bintz, R., Fuchs, R. P. & Cordonnier, A. M. (2007). Requirements for PCNA monoubiquitination in human cell-free extracts. *DNA Repair (Amst.)*, **6**, 1726–1731.
63. Bebenek, K., Matsuda, T., Masutani, C., Hanaoka, F. & Kunkel, T. A. (2001). Proofreading of DNA polymerase η-dependent replication errors. *J. Biol. Chem.* **276**, 2317–2320.
64. Acharya, N., Yoon, J. H., Gali, H., Unk, I., Haracska, L., Johnson, R. E. *et al.* (2008). Roles of PCNA-binding and ubiquitin-binding domains in human DNA polymerase η in translesion DNA synthesis. *Proc. Natl Acad. Sci. USA*, **105**, 17724–17729.
65. Parker, J. L., Bielen, A. B., Dikic, I. & Ulrich, H. D. (2007). Contributions of ubiquitin- and PCNA-binding domains to the activity of polymerase η in *Saccharomyces cerevisiae*. *Nucleic Acids Res.* **35**, 881–889.
66. Ouchida, R., Ukai, A., Mori, H., Kawamura, K., Dolle, M. E., Tagawa, M. *et al.* (2008). Genetic analysis reveals an intrinsic property of the germinal center B cells to generate A:T mutations. *DNA Repair (Amst.)*, **7**, 1392–1398.

Paternal monoenergetic neutron exposure results in abnormal sperm, and embryonal lethality and transgenerational tumorigenesis in mouse F_1 offspring

HIROMITSU WATANABE[1], MEGUMI TOYOSHIMA[1], MASAYORI ISHIKAWA[2] and KENJI KAMIYA[1]

[1]Department of Experimental Oncology, Research Institute for Radiation Biology and Medicine, Hiroshima University, Kasumi 1-2-3, Minami-ku, Hiroshima 734-8553; [2]Department of Molecular Trace Radiation Medicine, Hokkaido University Hospital, North 15 West 7, Kita-ku, Sapporo 060-8648, Japan

Received December 2, 2009; Accepted January 28, 2010

DOI: 10.3892/or_00000771

Abstract. Experiments were conducted to assay whether monoenergetic neutron-induced genetic damage in parental germline cells can give rise to development of cancer in the offspring. Seven-week-old C3H male mice were irradiated with monoenergetic neutrons with energy levels of 0.2 or 0.6 MeV at doses of 0, 50, 100 or 200 cGy. Two weeks after irradiation, when the male mice showed an increased incidence of sperm abnormalities, they were mated with virgin 9-week-old C57BL females. Litter size was decreased and embryo lethalities were increased in a dose-dependent manner. Furthermore, tumor incidence in male offspring born to male mice irradiated with 25 or 50 cGy at 0.6 MeV showed a tendency for increase as compared to the non-irradiated group value. Liver tumors in the 50 cGy group were significantly increased (P=0.03). It is concluded that the increased hepatic tumor risk in the F_1 generation may have been caused by genetic transmission of some hepatoma-associated trait(s) induced by monoenergetic neutron irradiation.

Introduction

There is now a wealth of information on the transmission of tumor-related genetic traits through germ cells from parents to offspring and research has been performed to address this question not only in man but also experimental animals (1-3). The possible importance of such genetic transmission is evidenced by the finding of increased risk of leukemia and non-Hodgkin lymphoma in children of workers at the Sellafield nuclear plant and in the West Berkshire and North Hampshine nuclear industries (4). Furthermore, experimental evidence for germinal transmission of cancer-related genetic damage has been obtained after parental exposure to ethylnitrosourea (5), X-rays and urethane (6) and neutron irradiation (7-9).

In order to study the radiobiological effects of neutron, the Hiroshima University Radiobiological Research Accelerator (HIRRAC) can be operated under conditions of high proton beam currents of 1 mA and acceleration voltages up to 3 MeV. The biological effects of monoenergetic neutrons are of particular interest to basic science and radiation protection (10). Concern is reflected in *in vitro* assays (11-17) as well as *in vivo* studies (18). To our knowledge, however, there has been relatively little work on the genetic effects of monoenergetic neutrons at various energy levels using *in vivo* systems.

Specifications for biological irradiation are presented in terms of monoenergetic beam conditions, dose rates and deposited energy spectra. High dose rates of monoenergetic neutron fields are useful for studying the neutron energy dependency of biological effects, and also for other radiobiology studies on the basic mechanisms of the effects of neutrons. Monoenergetic neutrons which have a narrow neutron spectrum are the most useful, therefore they were chosen for the present study of whether irradiation-induced genetic damage can be passed to the offspring, causing embryonic lethality and tumor development in the F_1 generation.

Materials and methods

Animals. COBOS male C3H/HeNCrj and female C57BL/6NCrj mice were purchased from Charles River Japan, Inc. (Hino, Japan) and housed in autoclaved cages on sterile wood chips, in a room with controlled temperature (24±2°C), humidity (55±10%) and a regular 12-h light, 12-h dark cycle, under the guidelines set forth in the 'Guide for the Care and Use of Laboratory Animals' established by Hiroshima University. They were fed a commercial diet MF (Oriental Yeast Co., Ltd., Tokyo, Japan) and were provided with normal tap water *ad libitum*. All experiments used the same lot of animals.

Correspondence to: Dr Hiromitsu Watanabe, Department of Experimental Oncology, Research Institute for Radiation Biology and Medicine, Hiroshima University, 1-2-3 Kasumi, Minami-ku, Hiroshima 734-8553, Japan
E-mail: tonko@hiroshima-u.ac.jp

Key words: monoenergetic neutrons, mouse, paternal exposure, offspring, tumorigenesis

Table I. Body, testis, epididymis weights and abnormal sperm induced 3 weeks after monoenegic neutron.

	BW	Testis	Epididymis	Testis/BW	Epi/bw	Sperm abnormal
0 cGy	28.9±1.9	0.17±0.02	0.063±0.006	6.01±0.76	2.21±0.20	1.56±0.76
0.2 MeV						
12.5 cGy	27.9±1.0	0.13±0.01[a]	0.062±0.007	4.69±0.47[a]	2.22±0.22	0.96±0.33
25 cGy	28.0±1.0	0.11±0.02[a]	0.056±0.004[a]	3.80±0.55[a]	2.01±0.16	1.93±1.08
50 cGy	27.9±1.3	0.10±0.01[a]	0.054±0.003[a]	3.46±0.17[a]	1.95±0.12[b]	1.92±1.18
100 cGy	26.7±1.2[a]	0.08±0.01[a]	0.053±0.005[a]	2.92±0.34[a]	1.97±0.23[b]	4.06±1.16[a]
		Y=-0.078X+0.14		Y=-0.026X+5.2		Y=0.026X+1.07
		r^2=-0.90		r^2=-0.89		r^2=0.92
		P<0.05		P<0.05		P<0.05
0.6 MeV						
12.5 cGy	27.7±1.1	0.13±0.01[a]	0.061±0.006	4.70±0.35[a]	2.19±0.20	1.50±0.65
25 cGy	29.3±1.9	0.11±0.01[a]	0.061±0.027	3.66±0.37[a]	2.10±0.21	2.36±1.66
50 cGy	28.0±1.3	0.09±0.01[a]	0.057±0.002[b]	3.36±0.33[a]	2.02±0.09	3.07±1.43[b]
100 cGy	27.5±1.1[b]	0.08±0.01[a]	0.055±0.005[a]	2.91±0.18[a]	1.98±0.20[b]	6.18±1.07[a,c]
		Y=-0.078X+0.14		Y=-0.026X+5.1		Y=0.048X+1.14
		r^2=-0.86		r^2=-0.84		r^2=0.98
						P<0.01

(Mean ± SD). [a]Significantly different from 0 cGy value (P<0.01). [b]Significantly different from 0 cGy value (P<0.05). [c]Significantly different from 0.2 MeV 100 cGy value (P<0.01).

Monoenergetic neutron irradiation. Neutron sources in this study was produced by Hiroshima University Radiobiological Research Accelerator (HIRRAC) as described previously (18). The HIRRAC can generate various monoenergetic neutrons using ^{7}Li(p,n)^{7}Be reaction with maximum accelerated voltage of 3 MV.

The absorbed doses were evaluated using paired ionization chambers IC-17 ATW (FWT, Inc., Goleta, CA, USA) and IC-17G (model GM539, FWT, Inc.). The IC-17ATW, which is made of tissue equivalent materials and filled with propane-base tissue equivalent gas, can measure the sum of neutron and γ-ray dose. The IC-17G, which is made of carbon and filled with carbon dioxide gas, can measure γ-ray dose with a few neutron dose contributions. Using these chambers, separate dose of neutron and γ-ray can be evaluated. The γ-ray contamination was estimated <3% of neutron dose when using 10-μm-thick lithium targets.

Each mouse was put into a box (3 cm x 3 cm x 5 cm) and 5 mice were located 20 cm away from target plane and 10 cm away from beam axis, which means that the mice were placed at 30 degrees direction position.

In order to uniform individual neutron doses, mice were rotated with a speed of 1 rpm. Groups of 5 mice were exposed by monoernergetic neutrons in 0.20 and 0.6 MeV (dose 50 cGy, dose rate 0.5 cGy/min) without anesthesia. The accelerated voltages for their neutron energy were 2.0 and 2.37 MV, respectively.

Experiments. One hundred and ten male mice received a single whole body exposure to monoernergetic neutrons with energy levels of 0.2 or 0.6 MeV at doses of 0, 25, 50, 100 or 200 cGy. Two weeks (spermatid stage) after irradiation, the males were mated with 3 non-irradiated 9-week-old C57BL female mice for a week, and retired males were then sacrificed. Testes were minced in saline and filtered and sperm were stained with Giemsa solution to allow the numbers of normal and abnormal sperm to be counted (19).

A total of 47 successfully mated females in one group were sacrificed 18 days after fertilization and the numbers of surviving and dead embryos were counted. In the remainder, offspring were obtained, the ratio of surviving pups was determined 1 week after birth, and the F_1 mice were maintained until 13.5 months of age.

Pathology. All animals were regularly observed on a daily basis and weighed once a month. At the time of necropsy, full autopsies were carried out under ether anesthesia, and body weights and various organ weights were determined. The number and size of liver tumor nodules were also measured and diseases of the liver and other organs including neoplastic changes were diagnosed by routine histological examination.

Statistical analysis. The significance of differences in numerical data was determined using the χ^2, Student's t-tests and the Dunnett method for multiple comparisons using logarithmic transformation.

Results

Changes in body and organ weights and appearance of abnormal sperm in the irradiated mice. Body weights of

Table II. Females mice used.

	Used females	Non-pregnancy	Pregnancy			
			Used for embryo lethality	Non-nursing	Nursing (%)	Total
0 cGy	37	15 (41)	4	1 (6)	17 (94)	18
0.2 MeV						
12.5 cGy	20	6 (30)	8	0	6 (100)	6
25 cGy	15	5 (33)	3	1 (14)	6 (86)	7
50 cGy	16	3 (19)	5	0	8 (100)	8
100 cGy	16	5 (31)	4	2 (29)	5 (71)	7
0.6 MeV						
12.5 cGy	19	7 (37)	7	1 (20)	4 (80)	5
25 cGy	20	4 (20)	8	1 (13)	7 (88)	8
50 cGy	15	5 (33)	3	0	7 (100)	7
100 cGy	37	16 (43)	5	11 (65)	6 (35)	17

100 cGy irradiated males with both energies were significantly decreased as compared with non-irradiated controls. Testis absolute (in 0.2 MeV Y=-0.078X+0.14, r^2=-0.90, P<0.05; in 0.6 MeV Y=-0.078X+0.14, r^2=-0.86) and relative weights (in 0.2 MeV Y=-0.026X+5.2, r^2=-0.89, P<0.05); in 0.6 MeV Y=-0.26X+5.1, r^2=-0.84) were also decreased linearly. The epididymis weights were decreased. Ratios of abnormal sperm were increased and with 100 cGy at 0.6 MeV the value was significantly greater than with 0.2 MeV (Table I) (0.2 MeV Y=0.026X+1.07, r^2=0.92, P<0.05; in 0.6 MeV Y=0.048X+1.14, r^2=0.98, P<0.01).

Survival of embryos. Data for used female mice are shown in Table II. Non-pregnant females accounted for 19-43%. Numbers of implantations per mouse were decreased in a dose-dependent manner (Table III 0.2 MeV Y=-0.035X+8.78, r^2=-0.91, P<0.05; in 0.6 MeV Y=-0.034X+93, r^2=-0.90, P<0.05). Numbers of total embryos in 100 cGy with both energy levels were significantly decreased as compared with other dose groups (Table III). Numbers of surviving embryos were significantly lower with 100 cGy irradiation with the average numbers of surviving embryos per mother were decreased in a dose-dependent manner (in 0.2 MeV Y=-0.058X+7.5, r^2=-0.99, P<0.01; in 0.6 MeV Y=-0.045X+7.6, r^2=-0.97, P<0.01). Conversely, lethality increased with the dose (in 0.2 MeV Y=0.02X+1.57, r^2=0.91, P<0.05; in 0.6 MeV Y=0.01X+1.71, r^2=0.65).

Table III. Mean survival data for embryos.

Group	Survival	Lethal	Total
0 cGy	7.50±1.00[a,c]	1.50±1.00	9.00±1.15a[a,c]
0.2 MeV			
12.5 cGy	6.50±1.20[a,c]	1.38±1.30	7.88±0.99[a,c]
25 cGy	5.00±2.00[b]	2.67±2.52	7.67±0.58[b]
50 cGy	5.20±2.28[a]	2.60±2.07	7.80±1.30[a,d]
100 cGy	1.50±1.29[e]	3.50±1.29	5.00±2.00[e]
	Y=-0.058X+7.5	Y=0.02X+1.57	Y=-0.035X+8.78
	r^2=-0.99, P<0.01	r^2=0.91, P<0.05	r^2=-0.91, P<.0.05
0.6 MeV			
12.5 cGy	7.43±1.72[a,c]	1.43±1.27	8.86±1.57[a,c]
25 cGy	5.75±2.05[a,d]	2.23±1.30	8.13±1.36[a,c]
50 cGy	5.67±0.58[a]	3.00±2.00	8.67±1.53[a,c]
100 cGy	3.00±1.22[e]	2.40±1.52	5.40±0.55[e]
	Y=-0.045X+7.6	Y=0.01X+1.71	Y=-0.034X+9.3
	r^2=0.97, P<0.01	r^2=0.65	r^2=-0.90, P<0.05

(Mean ± SD). [a]Significantly difference from 0.2 MeV 100 cGy value (P<0.01). [b]Significantly difference from 0.2 MeV 100 cGy value (P<0.05). [c]Significantly difference from 0.6 MeV 100 cGy value (P<0.01). [d]Significantly difference from 0.6 MeV 100 cGy value (P<0.05). [e]Significantly difference from 0 cGy value (P<0.01).

Birth rate and offspring nursing rate. Data for non-nursing mothers are given in Table II. The number was increased with 100 cGy at the 0.6 MeV energy level.

Offspring from mating two weeks after irradiation. Data for litter size and sex ratios are given in Table IV. Mean offspring number per mother was decreased dose-dependently at the 0.2 MeV energy level (total pups Y=-0.05X+8.3, r^2=-0.99, P<0.01; male Y=-0.03X+4.0, r^2=-0.96, P<0.01; female Y=-0.024X+4.2, r^2=-0.94, P<0.05) and with 0.6 MeV (total Y=-0.06X+8.0, r^2=-0.97, P<0.01; female Y=-0.04X+4.4, r^2=-0.86) except in males (Y=-0.01X+2.8, r^2=-0.57). The sex ratio at 0.2 MeV was about 50:50 but at 0.6 MeV differed with 12.5 cGy. In the long-term study, total number of offspring with 100 cGy at both energy levels was small.

Sequential assessment showed significant increase in body weights with 50 cGy at 0.2 MeV during 4-7 months and with 50 cGy at 0.6 MeV during to 12 months in males as

Table IV. Sex ratio after birth and effective animals.

Group	Sex ratio			No. of animals		
	Total	Male	Female	Total	Male (%)	Female (%)
0 cGy	8.53±1.37	4.53±1.37	3.88±1.73	138	74 (54)	64 (46)
0.2 MeV						
12.5 cGy	7.33±1.51	3.33±1.63	4.00±1.26	47	24 (51)	23 (49)
25 cGy	7.33±1.21	3.17±0.98	4.17±0.75	43	21 (49)	22 (51)
50 cGy	5.38±1.85[a]	2.63±0.92[a]	2.75±1.28	40	20 (50)	20 (50)
100 cGy	3.20±0.84[a]	1.40±0.89[a]	1.80±0.84[b]	16	7 (44)	9 (56)
	Y=-0.05X+8.3	Y=-0.03X+4.0	Y=-0.024X+4.22			
	r^2=-0.99, P<0.01	r^2=-0.96, P<0.01	r^2=-0.94, P<0.05			
0.6 MeV						
12.5 cGy	7.50±1.9	2.50±2.38[b]	5.00±2.16	29	10 (34)	19 (66)
25 cGy	6.00±1.63[a]	2.29±1.25[a]	3.71±1.60	38	16 (42)	22 (58)
50 cGy	4.43±0.98[a]	3.14±1.21	1.29±1.11[a]	42	22 (52)	20 (48)
100 cGy	2.50±1.22[a]	1.50±0.84[a]	1.00±0.63[a]	17	8 (47)	9 (53)
	Y=-0.06X+8.0	Y=-0.01X+2.8	Y=-0.04X+4.4			
	r^2=-0.97, P<0.01	r^2=-0.57	r^2=-0.86			

(Mean ± SD). [a]Significantly different from 0 cGy value (P<0.01). [b]Significantly different from 0 cGy value (P<0.05).

Table V. Body weights of F_1 male mice.

Group	3 months	4 months	5 months	6 months	7 months	8 months	9 months	10 months	11 months	12 months	13 months	14.5 months
0 cGy	32.1±2.7	34.2±3.4	38.2±4.0	40.0±3.9	40.8±4.2	42.7±1.9	44.3±3.4	45.2±3.1	46.2±3.3	46.8±3.6	46.8±3.4	46.0±3.4
0.2 MeV												
12.5 cGy	30.7±2.9	32.8±3.5	35.4±4.5[b]	37.1±4.9[b]	39.2±5.1	41.0±5.0	42.3±4.7	43.5±4.3	44.6±4.0	45.8±4.0	45.6±3.1	45.1±3.8
25 cGy	30.8±2.5	33.0±3.4	36.1±4.3	37.0±4.1[b]	38.3±4.3[b]	40.0±4.2[b]	41.3±4.2[a]	42.5±4.0[b]	43.6±4.0[b]	44.4±4.1[b]	45.2±4.1	44.5±4.1
50 cGy	33.8±2.7	37.5±3.6[a]	40.8±3.2[b]	42.1±3.1[b]	43.4±2.9[b]	44.2±2.7	45.2±2.9	46.0±3.0	47.3±3.1	48.1±2.9	48.1±3.9	47.6±3.2
100 cGy	32.5±0.9	34.8±2.0	38.0±3.2	41.6±4.5	44.2±4.5	45.7±2.9	47.0±2.7	47.2±2.2	48.4±1.8	48.6±1.7	46.6±3.9	45.2±2.2
0.6 MeV												
12.5 cGy	31.7±1.4	33.8±2.5	37.4±3.0	38.5±3.1	41.4±4.1	41.9±3.2	43.3±3.1	44.2±2.1	45.8±2.0	46.5±3.0	46.0±3.4	45.0±3.8
25 cGy	31.7±2.3	35.1±3.1	38.5±3.9	40.4±3.0	42.7±3.5	43.9±2.8	45.7±2.8	46.7±2.8	47.9±2.9	48.3±3.3	48.8±3.6	48.1±4.0
50 cGy	32.1±4.2	36.8±4.3[b]	41.1±4.1[b]	42.8±3.8[a]	44.2±3.1[a]	46.1±3.0[a]	47.4±3.4[a]	47.7±4.5[b]	49.6±3.8[a]	49.2±3.7[b]	48.9±3.5	47.8±3.4
100 cGy	31.6±4.1	34.9±5.5	38.6±5.9	40.0±5.7	40.4±5.1	42.2±5.7	43.4±5.5	44.0±6.2	45.6±6.0	45.4±5.3	46.2±5.9	45.3±5.6

(Mean ± SD). [a]Significantly different from 0 cGy value (P<0.01). [b]Significantly different from 0 cGy value (P<0.05).

compared to control males (Table V), whereas significantly decrease was evident with 25 cGy at 0.2 MeV. Female body weights were significantly heavier than for controls with 50 cGy at 0.2 MeV from 3 to 6 months, with 100 cGy at 0.2 MeV during the whole experiment, with 25 cGy at 0.6 MeV from 5 to 12 months, and with 50 cGy at 0.6 MeV from 5 to 13.5 months, whereas with 25 cGy they were decreased from 8 to 13.5 months as compared with control values (Table VI).

At autopsy, body weights of male F_1 mice of the 0.2 MeV energy level groups were not significantly altered (Table VII). Testis weights with 100 cGy were significantly lower than the non-irradiated group whereas adrenals were heavier. Relative testis weights (organ weight/body weight x1000) with 50 and 100 cGy were also significantly decreased as compared with the non-irradiated group and again adrenal values were increased (Table VIII).

Table VI. Body weights of F_1 female mice.

Group	3 months	4 months	5 months	6 months	7 months	8 months	9 months	10 months	11 months	12 months	13 months	14.5 months
0 cGy	24.2±1.4	26.0±1.9	27.0±3.2	29.6±3.5	32.0±4.4	34.2±5.1	36.2±5.8	37.6±6.2	40.8±6.0	42.8±6.0	43.6±6.1	43.1±6.4
0.2 MeV												
12.5 cGy	24.7±2.0	26.0±2.3	27.9±2.9	30.2±3.3	31.1±3.6	33.9±4.3	35.8±4.4	38.0±5.1	41.1±6.2	41.9±6.8	42.8±7.2	42.8±7.1
25 cGy	24.1±1.5	25.4±2.1	27.1±2.9	28.3±2.7	30.0±2.8	30.7±3.1[b]	32.7±3.6[b]	33.6±3.7[b]	36.5±4.2[b]	37.9±4.4[a]	37.6±4.7[a]	38.3±4.6[b]
50 cGy	26.0±2.1[b]	28.6±4.2[a]	30.0±3.6[a]	32.6±4.4[b]	34.3±5.2	36.4±5.8	38.2±5.4	40.3±6.7	43.7±6.0	46.2±5.8	47.1±5.6	44.4±9.3
100 cGy	27.8±3.0[a]	31.0±3.2[a]	33.9±3.9[a]	36.6±3.3[a]	38.5±5.2[a]	40.3±4.2[a]	42.3±4.1[a]	44.0±3.4[a]	47.4±3.7[a]	49.9±2.8[a]	50.0±3.0[b]	48.9±3.5[b]
0.6 MeV												
12.5 cGy	24.5±1.8	25.8±3.2	28.4±3.6	29.7±4.2	31.5±4.3	35.1±6.1	38.3±6.3	38.3±6.7	40.7±6.9	41.0±6.7	40.7±6.9	39.6±6.9
25 cGy	24.6±2.3	27.1±2.9	31.3±4.9[a]	33.2±5.2[a]	35.4±5.2[a]	38.4±6.0[a]	40.9±6.0[a]	42.3±6.1[a]	45.3±6.3[a]	46.4±6.2[b]	45.8±10.9	47.4±6.6
50 cGy	24.7±1.3	27.7±2.4	32.3±3.4[a]	35.2±3.4[a]	38.9±3.2[a]	41.4±4.8[a]	44.6±4.5[a]	44.9±4.9[a]	48.8±6.2[a]	49.2±5.3[a]	49.8±5.2[b]	48.6±5.9[b]
100 cGy	26.5±2.5[b]	24.8±11.4	31.9±6.0[a]	34.0±7.1[b]	35.7±7.4	38.0±7.4	40.0±8.4	42.2±8.8	45.7±9.0	46.0±8.1	47.3±9.9	46.3±9.1

(Mean ± SD). [a]Significantly different from 0 cGy value (P<0.01). [b]Significantly different from 0 cGy value (P<0.05).

Table VII. Body and organ weight for F_1 male.

Group	Body weight	Liver	Kidney	Testis	Adrenal	Spleen
0 cGy	46.0±3.4	2.15±0.36	0.61±0.07	0.21±0.01	0.007±0.002	0.11±0.03
0.2 MeV						
12.5 cGy	45.1±3.8	2.20±0.33	0.62±0.07	0.20±0.02	0.006±0.001	0.10±0.03
25 cGy	44.5±4.1	2.05±0.28	0.59±0.08	0.20±0.03	0.006±0.001	0.10±0.02
50 cGy	47.6±3.2	2.30±0.36	0.63±0.09	0.20±0.002	0.007±0.002	0.12±0.06
100 cGy	45.2±2.2	2.19±0.38	0.58±0.04	0.18±0.05[b]	0.026±0.042[a]	0.13±0.12
0.6 MeV						
12.5 cGy	45.0±3.8	2.00±0.24	0.62±0.09	0.21±0.01	0.007±0.002	0.10±0.01
25 cGy	48.1±4.0	2.52±0.58	0.69±0.07[a]	0.21±0.02	0.009±0.002	0.12±0.05
50 cGy	47.8±3.4	2.27±0.38	0.61±0.05	0.19±0.05[b]	0.008±0.001	0.12±0.03
100 cGy	45.3±5.6	2.22±0.63	0.57±0.12	0.18±0.03[b]	0.008±0.003	0.11±0.03

(Mean ± SD). [a]Significantly different from 0 cGy value (P<0.01). [b]Significantly different from 0 cGy value (P<0.05).

Body and kidney weights with 25 cGy at the 0.6 MeV energy level were increased, along with the relative liver and kidney weights in 25 cGy were heavier than non-irradiated group but testis in 50 cGy was decreased.

Table IX summarizes data for tumors in male F_1 offspring. Most lesions were liver tumors. Incidences overall were 25.7, 8.3 4.8, 25.0 and 42.9% with 0, 12.5, 25, 50 and 100 cGy at the 0.2 MeV energy level, respectively, and 0, 37.5, 45.5 and 25% at 0.6 MeV. Incidences of liver tumors were 18.9, 8.3, 4.8, 25.0 and 28.6 % at the 0.2 MeV energy level, respectively, and 0, 31.3, 40.1 (P=0.03) and 25% at 0.6 MeV. Sizes and number of liver tumors did not significantly differ among the groups.

Female mouse body and organ weights are shown in Table X. Body weights with 25 cGy at 0.2 MeV were significantly decreased as compared with the non-irradiated group, and ovary and adrenal weights were significantly increased with 100 cGy and liver and kidney weights with 25 and 50 cGy. Relative adrenal weights with 12.5 cGy and liver with 100 cGy were significantly decreased whereas ovary values were elevated at 100 cGy (Table XI).

Regarding incidences of tumors in females, three tumors (4.7%, hemangioma, lymphoma and ovary) appeared in the non-irradiated group, and values were 3/23 (13%, hepatoma, lung and ovary tumors), 3/22 (14%, ovary tumor), 1/20 (5%, ovary tumor) and 0 in the 12.5, 25, 50 and 100 cGy groups at

Table VIII. Relative organ weight for F_1 male mice.

Group	Liver	Kidney	Testis	Adrenal	Spleen
0 cGy	46.7±7.2	13.3±1.1	4.5±0.3	0.16±0.04	2.5±0.7
0.2 MeV					
12.5 cGy	48.8±6.1	13.8±0.9	4.3±0.4	0.14±0.03	2.2±0.6
25 cGy	46.1±3.2	13.3±1.4	4.5±0.6	0.14±0.03	2.3±0.4
50 cGy	48.3±5.8	13.3±1.4	4.1±0.8[b]	0.15±0.03	2.5±1.3
100 cGy	48.5±7.8	12.8±1.1	3.9±1.0[b]	0.59±0.93[a]	3.2±3.0
0.6 MeV					
12.5 cGy	44.3±2.4	13.7±1.7	4.6±0.4	0.17±0.05	2.2±0.3
25 cGy	52.0±9.6[b]	14.5±0.9[a]	4.3±0.4	0.18±0.05	2.5±1.1
50 cGy	47.2±5.7	12.9±0.9	4.0±1.1[a]	0.17±0.03	2.5±0.5
100 cGy	48.2±9.1	12.6±1.4	4.1±0.7	0.17±0.05	2.4±0.5

(Mean ± SD). [a]Significantly different from 0 cGy value ($P<0.01$). [b]Significantly different from 0 cGy value ($P<0.05$).

Table IX. Incidence of tumors for F_1 male mice.

Group	Effective no. of animal	Tumor bearing animal	Incidence	Liver tumor size	No. of liver tumor per mouse	Other tumor
0 cGy	74	19 (25.7)	14 (18.9)	1.59±4.13	0.20±0.40	Lung papilloma
0.2 MeV						
12.5 cGy	24	2 (8.3)	2 (8.3)	1.04±3.53	0.08±0.28	
25 cGy	21	1 (4.8)	1 (4.8)	0.24±1.09	0.05±0.22	
50 cGy	20	5 (25.0)	5 (25.0)	1.57±3.45	0.35±0.67	
100 cGy	7	3 (42.9)	2 (28.6)	2.13±4.16	0.57±0.79	Hemangioma
0.6 MeV						
12.5 cGy	10	0	0	0	0	
25 cGy	16	6 (37.5)	5 (31.3)	4.18±7.03	0.38±0.62	Harderian
50 cGy	22	10 (45.5), P=0.08	9 (40.1)[a], P=0.03	1.23±2.19	0.59±0.85	Hemangioma
100 cGy	8	2 (25)	2 (25)	2.33±4.69	0.38±0.74	

(Mean ± SD).

the 0.2 MeV energy level, respectively. The figures were 0, 5/22 (22.7), 5/20 (25%, ovary tumor) and 1/9 (11.1%, ovary) at the 0.6 MeV energy level (Table XII).

Discussion

The present experiments showed clear increase in the incidence of abnormal sperm in C3H males following monoenergetic neutron irradiation, resulting in increased embryo lethality of F_1 offspring and liver tumors in surviving F_1 males. While the sperm abnormalities were energy dose-dependent, this did not appear to be the case for embryonic death and tumor incidence.

This lack of dose-dependence is in line with the literature. Inverse dose-dependence for fission spectrum neutron induction of somatic hprt deficiency mutations has been reported by Nakamura and Sawada (20) with mouse leukemia L5178Y cells and ^{252}Cf-fission neutrons. Brenner and Hall published an inverse dose effect model for neoplastic transformation *in vitro* following high LET irradiation (21). Furthermore, Zhang *et al* (17) reported different doses of neutrons to produce approximately linear changes in the frequency of micronuclei in root-tip cells of *Allium cepaonion* irradiated as either dry dormant seeds or seedlings. Balcer-Kubiczek *et al* (22) earlier found modification of fission neutron dose-response curves on varying the dose rate to be negligible or

Table X. Body and organ weight for F_1 female mice.

Group	Body weight	Liver	Kidney	Ovary	Uterus	Adrenal	Spleen
0 cGy	43.1±6.4	1.60±0.28	0.36±0.03	0.026±0.023	0.478±0.541	0.026±0.023	0.110±0.022
0.2 MeV							
12.5 cGy	42.8±7.1	1.63±0.22	0.37±0.04	0.022±0.005	0.378±0.124	0.022±0.005	0.108±0.024
25 cGy	38.3±4.6[b]	1.46±0.17	0.36±0.04	0.026±0.005	0.580±0.472	0.026±0.006	0.110±0.030
50 cGy	44.4±9.3	1.62±0.37	0.38±0.04	0.026±0.007	0.509±0.176	0.026±0.007	0.120±0.054
100 cGy	48.9±3.5[b]	1.62±0.23	0.40±0.05	0.070±0.138[a]	0.299±0.160	0.070±0.138[a]	0.129±0.052
0.6 MeV							
12.5 cGy	39.6±6.9	1.58±0.30	0.38±0.05	0.029±0.010	0.662±0.509	0.028±0.009	0.119±0.039
25 cGy	47.4±6.6	1.77±0.30[b]	0.40±0.06[a]	0.033±0.033	0.488±0.479	0.033±0.033	0.122±0.029
50 cGy	48.6±5.9[b]	1.95±0.33[a]	0.44±0.04[a]	0.021±0.006	0.742±0.828	0.021±0.006	0.120±0.023
100 cGy	46.3±9.1	1.69±0.48	0.37±0.08	0.058±0.088	0.256±0.171	0.058±0.088	0.103±0.042

(Mean ± SD). [a]Significantly different from 0 cGy value ($P<0.01$); [b]Significantly different from 0 cGy value ($P<0.05$).

Table XI. Relative body weight for F_1 female.

Group	Liver	Kidney	Ovary	Uterus	Adrenal	Spleen
0 cGy	37.3±5.4	8.59±1.22	0.606±0.495	11.85±17.04	0.237±0.186	2.85±1.02
0.2 MeV						
12.5 cGy	38.4±4.6	8.88±1.09[b]	0.525±0.168	9.16±3.75	0.205±0.057[b]	2.60±0.88
25 cGy	38.4±3.7	9.43±1.15	0.683±0.208	15.47±12.24	0.390±0.576	2.88±0.77
50 cGy	35.0±6.4	8.23±0.68	0.553±0.152	11.17±4.02	0.202±0.054	2.56±0.86
100 cGy	33.1±3.0[b]	8.15±0.90	1.375±2.649[b]	6.08±3.13	0.197±0.050	2.61±0.95
0.6 MeV						
12.5 cGy	40.1±4.5	9.74±1.45[a]	0.727±0.234	18.35±17.00	0.267±0.078	3.06±0.95
25 cGy	37.6±3.7	8.52±1.41	0.721±0.734	10.71±10.57	0.235±0.072	2.62±0.71
50 cGy	40.1±3.4	9.06±0.73	0.445±0.134	16.58±20.65	0.171±0.027	2.47±0.36
100 cGy	36.4±5.3	8.05±0.59	1.188±1.756	5.33±3.39	0.192±0.055	2.23±0.65

(Mean ± SD). [a]Significantly different from 0 cGy value ($P<0.01$). [b]Significantly different from 0 cGy value ($P<0.05$).

absent. On the other hand, Hill and Williams-Hill (23) observed that reduction of the dose rate of fission neutrons increases their effectiveness for transformation of C3H 10T1/2 cells. Watanabe *et al* (24) reported that a single ^{252}Cf neutron dose resulted in higher incidences of ovarian and Harderian gland tumors than the same total dose given at a low dose rate with B6C3F1 mouse whole body irradiation. Clearly there may be differences between the *in vitro* and *in vivo* situations. It is considered that cells with large chromosomal aberrations or other abnormalities might be able to survive *in vitro*, but *in vivo* they might not, so smaller non-lethal chromosomal changes such as point mutations, frame shifts, as small additions or deletions could be essential for tumor induction *in vivo*. The source of irradiation, strain, sex, age and plants or animals are all clearly factors which need to be taken into account when determining radiation sensitivity. Recently, we reported that there were no significant differences in the tumor induction rate among the different energy such as 0.18, 0.32, 0.6 and 1.0 MeV monoenergetic neutron irradiation (18). Sasaki *et al* (25) also mentioned that induction of chromosome aberrations is not clearly dependent on neutron energy. In conclusion, there have been no consistent differences in tumor incidence among the various energies of neutron irradiation applied.

Goud *et al* (26) reported that exposure of mice to ^{252}Cf neutrons and gamma rays resulted in a decrease in testis weight and a concomitant increase in frequency of abnormal sperm. According to Hugenholtz and Bruce (19) X-ray-

Table XII. Incidence of tumor for F_1 female mice.

Group	Effective no. of animal	Positive (%)	Type of tumor
0 cGy	64	3 (4.7)	Hemangioma, lymphoma, ovary
0.2 MeV			
12.5 cGy	23	3 (13.0)	Hepatoma, lung, ovary
25 cGy	22	3 (13.6)	Ovary 3
50 cGy	20	1 (5.0)	Ovary
100 cGy	9	0	
0.6 MeV			
12.5 cGy	19	0	
25 cGy	22	5 (22.7)	Hepatoma, lymphoma, ovary 2, sarcoma
50 cGy	20	5 (25.0)	Ovary 5
100 cGy	9	1 (11.1)	Ovary

induced abnormalities in sperm are transmissible up to the F_2 generation as dominant mutations. Nomura (27,28) demonstrated an increase in the dominant lethality and congenital malformations in offspring of male or female mice irradiated with X-rays (6) or treated with urethane (27,28). These findings were further confirmed by Kirk and Lyon (29), West *et al* (30) and Lyon and Renshaw (31), using the same dose but different strains of mice. Nomura (6) also reported increased fetal death of F_1 offspring after paternal irradiation at the stage of spermatozoa and spermatids in a dose-dependent manner. Kurishita *et al* (32) demonstrated that external abnormalities are induced in offspring of male mice following treatment of germ cells at the spermatogonia stage with ^{252}Cf neutrons and the dose-response curve was linear up to 0.95 cGy. Streffer (33) similarly observed that a transgenerational transmission occurs for ionizing radiation-induced congenital malformations as well as for genomic instability, the latter measured at the chromosome level. Carls *et al* (34) described that ionizing radiation exposure of the germline can induce delayed DNA deletions in offspring mice. They suggested that DNA deletion events are implicated in the onset of carcinogenesis and a similar phenomenon in humans may account for a portion of childhood cancers. Nomura (6) found the incidence of tumors in F_1 mice of the ICR strain to increased, in this case dose-dependently, after paternal exposure to 36, 216 or 364 cGy of X-rays at the stage of spermatozoa, spermatids or spermatogonia. Of the tumors occurring in the F_1 offspring, 90% were lung tumors. Daher *et al* (35) reported that paternal X-ray irradiation resulted in reduction of litter size and a marginally significant doubling of the leukemia/lymphoma rate in the offspring in N5 strain mice, over a 1 year observation period. Urethane treatment of F_1 offspring derived from irradiated parents caused a 2.4 times greater incidence of tumors than observed in untreated controls (36). Vorobtsova *et al* (37) reported similar results with a different mouse strain. Mewissen *et al* (38) found that repeated administration of ^3H_2O as the drinking water to C57BL/6M males before mating over several generations gave rise to hereditary adenocarcinomas in the small intestine. Essentially comparable effects of chemical carcinogens have been reported (39-41). A high incidence of liver tumors was observed in the F_1 offspring of C3H male mice which had been exposed to 50 cGy of ^{252}Cf neutrons and mated with C57BL/6 females (8,9). In the present experiment, similar results were observed with 50 cGy especially at the 0.6 MeV energy level. Shay *et al* (42) documented that when 35- to 46-day-old Wistar rat females were treated with 3-methylcholanthrene using gastric tubes every day for two months and then mated with untreated males, the incidence of cancer was increased significantly in F_1 and F_2 offspring. Tomatis *et al* (5) subsequently found in the BDV1 rat system that the incidence of nerve tumors was significantly elevated in the F_1 generation when mating occurred two weeks after treatment of 9-week-old male rats with 80 mg/kg of ethylnitrosourea. Dasenbrock *et al* (43) described that maternal preconceptual exposure in C57BL/6J mice to radiation is associated with a moderately increased incidence of liver and lung tumors in the male descendants. The incidence of total tumors in the F_1 offspring, however, was not different from the control value. Lord *et al* (44) reported that with methylnitrosourea following preconceptional paternal contamination with ^{239}plutonium the second generation excess of leukemia appears to be the result of preconceptional paternal irradiation and may be related to inherited changes that affect the development of haemopoietic stem cells. The evidence in humans is most derived from case reports and epidemiological studies of consequences to the progeny of paternal occupational exposure to chemicals, ionizing radiation and electromagnetic fields prior to conception (3,45-47). Dasenbrock *et al* (43) indicated that maternal preconceptual X-ray exposure to radiation is associated with a moderately increased incidence of liver and lung tumors in male descendants in C57BL/6N mice. Thus the fact that genetic damage to parental germ cells can be transmitted to the offspring as an origin of carcinogenesis has been well documented, and this was confirmed in the present experiment.

However, Cattanach *et al* (48) described no significant increase but seasonal changes in the incidence of lung tumors in offspring of BALB/cJ or C3H/Heh mice exposed to X-rays following the experimental protocol of Nomura (6). Evidence for such seasonal changes in tumor incidence has been published and this relates to experiments carried out in insufficiently controlled animal facilities and experimental conditions, e.g., animals exposed to outdoor light. In fact, change of the light-dark interval significantly influences tumor frequencies in mice (49). Cattanach *et al* (48) also reported that reduction in litter size in paternally irradiated groups might be evidence of genetic damage, i.e., dominant lethality, resulting from the radiation exposure.

As a general rule, heavier mice are more likely to develop spontaneous and induced tumors earlier and caloric restriction decreases body weights and tumor incidences and increases longevity. Selby *et al* (50) suggested that induced dominant lethality in mice or rats with increased tumor rates have no relation with induction of dominant tumor mutations. In the

present experiment numbers of offspring were lower with 100 cGy at both energy levels and the fact that only a few animals survived means that the incidence of liver tumors might not have been accurate. The range of gene damage is presumably very wide, given the sperm abnormalities and the embryo lethality and malformations, and many embryos died, so that surviving animals might have been those less susceptible to induction of tumors. However, if gene damage is limited, tumor-prone animals might survive, resulting in greater causation of tumors. Nomura suggested that germ-line exposure is a very early tumorigenesis by itself. It is possible that the lack of increase in lung tumors reported by Cattanach *et al* (48) may be attributable to increased incidence of embryo lethality caused by high doses of paternal X-ray irradiation.

In conclusion, the results of the present study indicate that paternal exposure to radiation is associated with an increased incidence of liver tumors in the male descendants. While our study was not designed to investigate the mechanism of transmission of increased risk, the results are in keeping with the hypothesis of a germ line-transmitted hereditary effect of monoenergetic neutron irradiation.

Acknowledgements

We are grateful to Professor T. Nomura, Osaka University, and to Dr M.A. Moore for critical reading of this manuscript, and Mr. T. Nishioka for technical assistance.

References

1. Napalkov NP, Rice JM, Tomatis L and Yamasaki H: Perinatal and multigeneration carcinogenesis. IARC Scientific Publication, Lyon, 96, 1989.
2. Tomatis L, Narod S and Yamasaki H: Transgeneration transmission of carcinogenic risk. Carcinogenesis 13: 145-151, 1992.
3. Tomatis L: Transgeneration carcinogenesis: a review of the experimental and epidemiological evidence. Jpn J Cancer Res 85: 443-454, 1994.
4. Gardner MJ, Snee MP, Hall AJ, Powell CA, Downes S and Terrell JD: Results of the case-control study of leukemia and lymphoma among young people near Sellafield nuclear plant in West Cumbria. Br Med J 300: 423-429, 1990.
5. Tomatis L, Cabral JRP, Likhachev AJ and Ponomrkov V: Increased cancer incidence in the progeny of male rats exposed to ethylnitrosourea before mating. Int J Cancer 28: 475-478, 1981.
6. Nomura T: Parental exposure to X rays and chemicals induces heritable tumors and anomalies in mice. Nature 296: 575-577, 1982.
7. Takahashi T, Watanabe H, Dohi K and Ito A: ^{252}Cf relative biological effectiveness and inheritable effect of fission neutrons in mouse liver tumorigenesis. Cancer Res 52: 1948-1953, 1992.
8. Watanabe H, Takahashi T, Lee JY, *et al*: Influence of paternal ^{252}Cf neutron exposure on abnormal sperm, embryonal lethality, and liver tumorigenesis in the F1 offspring of mice. Jpn J Cancer Res 87: 51-57, 1996.
9. Shoji S, Masaoka Y, Kurosumi M, Katoh O and Watanabe H: Tumorigenesis in F_1 offspring mice following paternal 12.5 cGy ^{252}Cf fission neutron irradiation. Oncol Rep 5: 1175-1178, 1998.
10. Miller RC, Marino SA, Martin SG, *et al*: Neutron-energy-dependent cell survival and oncogenic transformation. J Radiat Res (Tokyo) (Suppl) 40: 53-59, 1999.
11. Pandita TK and Geard CR: Chromosome aberrations in human fibroblasts induced by monoenergetic neutrons. I. Relative biological effectiveness. Radiat Res 145: 730-739, 1996.
12. Kubota N, Okada S, Nagatomo S, *et al*: Mutation induction and RBE of low energy neutrons in V79 cells. J Radiat Res (Tokyo) (Suppl) 40: 21-27, 1999.
13. Tanaka K, Gajendiran N, Endo S, Komatsu K, Hoshi M and Kamada N: Neutron energy-dependent initial DNA damage and chromosomal exchange. J Radiat Res (Tokyo) (Suppl) 40: 36-44, 1999.
14. Tanaka K, Kobayashi T, Sakurai Y, Nakagawa Y, Endo S, Hoshi M: Dose distributions in a human head phantom for neutron capture therapy using moderated neutrons from the 2.5 MeV proton-^{7}Li reaction or from fission of ^{235}U. Phys Med Biol 46: 2681-2695, 2001.
15. Gajendiran N, Tanaka K and Kamada N: Comet assay to sense neutron 'fingerprint'. Mutat Res 452: 179-187, 2000.
16. Schmid E, Schlegel D, Guldbakke S, Kapsch RP and Regulla D: RBE of nearly monoenergetic neutrons at energies of 36 keV-14.6 MeV for induction of dicentrics in human lymphocytes. Radiat Environ Biophys 42: 87-94, 2003.
17. Zhang W, Fujikawa K, Endo S, Ishikawa M, Ohtaki M, Ikeda H and Hoshi M: Energy-dependent RBE of neutrons to induce micronuclei in root-tip cells of *Allium cepa* onion irradiated as dry dormant seeds and seedlings. J Radiat Res (Tokyo) 44: 171-177, 2003.
18. Watanabe H, Kashimoto N, Kajimura J, Ishikawa M and Kamiya K: Tumor induction by monoenergetic neutrons in B6C3F1 mice. J Radiat Res (Tokyo) 48: 205-210, 2007.
19. Hugenholtz AP and Bruce WR: Radiation induction of mutations affecting sperm morphology in mice. Mutat Res 107: 177-185, 1983.
20. Nakamura N and Sawada S: Reversed dose-rate effect of RBE of ^{252}calfornium radiation in the induction of 6-thioguanine-resistant mutations in mouse L5176Y cells. Mutat Res 201: 65-71, 1988.
21. Brenner DJ and Hall EJ: The inverse dose-rate effect for oncogenic transformation by neutrons and charged particles: a plausible interpretation consistent with published data. J Radiat Biol 58: 745-758, 1990.
22. Balcer-Kubiczek EK, Harrison GH, Hill CK and Blakely WF: Effects of WR-1065 and WR-151326 on survival and neoplastic transformation in C3H/10T1/2 cells exposed to TRIGA or JANUS fission neutrons. Int J Radiat Biol 63: 37-46, 1993.
23. Hill CK and Williams-Hill D: Neutron carcinogenesis: past, present and future. J Radiat Res (Tokyo) (Suppl) 40: 117-127, 1999.
24. Watanabe H, Okamoto T, Yamada K, *et al*: Effects of dose rate and energy level on fission neutron (^{252}Cf) tumorigenesis in B6C3F1 mice. J Radiat Res (Tokyo) 34: 235-239, 1993.
25. Sasaki MS, Endo S, Ejima Y, *et al*: Effective dose of A-bomb radiation in Hiroshima and Nagasaki as assessed by chromosomal effectiveness of spectrum energy photons and neutrons. Radiat Environ Biophys 45: 79-91, 2006.
26. Goud SN, Feola JM and Maruyama Y: Sperm shape abnormalities in mice exposed to californium-252 radiation. Int J Radiat Biol 52: 755-760, 1987.
27. Nomura T: Transmission of tumors and malformations to the next generation of mice subsequent to urethan treatment. Cancer Res 35: 264-266, 1975.
28. Nomura T: Transgenerational effects from exposure to environmental toxic substances. Mutat Res 659: 185-193, 2008.
29. Kirk M and Lyon MF: Induction of congenital malformations in the offspring of male mice treated with X-rays at pre-meitic and post-meiotic stages. Mutat Res 125: 75-85, 1984.
30. West JD, Kirk Y, Goyder Y and Lyon MF: Discrimination between the effects of X-ray irradiation of the mouse oocyte and uterus on the induction of dominant lethals and congenital anomalies. I. Embryo-transfer experiments. Mutat Res 149: 221-230, 1985.
31. Lyon MF and Renshaw R: Induction of congenital malformations in mice by parental irradiation: transmission to later generations. Mutat Res 198: 277-283, 1988.
32. Kurishita A, Ono T, Okada S, Mori Y and Sawada S: Induction of external abnormalities in offspring of male mice irradiated with ^{252}Cf neutron. Mutat Res 268: 323-328, 1992.
33. Streffer C: Transgenerational transmission of radiation damage: genomic instability and congenital malformation. J Radiat Res (Tokyo) (Suppl B) 47: B19-B24, 2006.
34. Carls Nand Schiestl RH: Effect of ionizing radiation on transgenerational appearance of p(un) reversions in mice. Carcinogenesis 20: 2351-2354, 1999.
35. Daher A, Varin M, Lamontagne Y and Oth D: Effect of preconceptional external or internal irradiation of N5 male mice and the risk of leukemia in their offspring. Carcinogenesis 19: 1553-1558, 1998.

36. Nomura T: X-ray-induced germ-line mutation leading to tumors. Its manifestation in mice given urethane post-natally. Mutat Res 121: 59-65, 1983.
37. Vorobtsova IE and Kitaev EM: Urethane-induced lung adenomas in the first-generation progeny of irradiated male mice. Carcinogenesis 11: 1931-1934, 1988.
38. Mewissen J, Ugarte AS and Rust JH: Tumeur intestinale hereditaire observé après irradiation de generations multiples d'une lignee germinale male de la souris C57BL/6. CR Soc Biol 178: 230-235, 1984.
39. Strong LC: Genetic analysis of the induction of tumors by methylcholanthrene. Am J Cancer Inst 39: 347-349, 1940.
40. Strong LC: Genetic analysis of the induction of tumors by methylcholanthrene. IX. Induced and spontaneous adenocarcinomas of the stomach in mice. J Natl Cancer Inst 5: 339-362, 1940.
41. Boutwell RK: Some biological aspects of skin carcinogenesis. Prog Exp Tumor Res 4: 207-250, 1964.
42. Shay H, Gruenstein M and Weinberger M: Tumor incidence in F_1 and F_2 generations derived from female rats fed methylcholanthrene by stomach tube prior to conception. Cancer Res 12: 296, 1952.
43. Dasenbrock C, Tillmann T, Ernst H, *et al*: Maternal effects and cancer risk in the progeny of mice exposed to X-rays before conception. Exp Toxicol Path 56: 351-360, 2005.
44. Lord BI, Woolford LB, Wang L, *et al*: Induction of lymphohaemopoietic malignancy: impact of preconception paternal irradiation. Int J Radiat Biol 74: 721-728, 1998.
45. Savitz DA and Chen JH: Parental occupation and childhood cancer: review of epidemiologic studies. Env Health Per 88: 325-337, 1990.
46. O'Leary LM, Hicks AM, Peters JM and London S: Parental occupational exposures and risk of childhood cancer: a review. Am J Ind Med 20: 17-35, 1991.
47. Pearce MS, Hammal DM, Dorak MT, McNally RJ and Parker L: Paternal occupational exposure to electro-magnetic fields as a risk factor for cancer in children and young adults: a case-control study from the North of England. Ped Blood Cancer 49: 280-286, 2007.
48. Cattanach BM, Patrick G, Papworth D, *et al*: Investigation of lung tumour induction in BALB/cJ mice following paternal X-irradiation. Int J Radiat Biol 67: 607-615, 1995.
49. Nakajima H, Narama I, Matsuura T and Nomura T: Enhancement of tumor growth under short light/dark cycle in mouse lung. Cancer Lett 78: 127-131, 1994.
50. Selby PB, Earhart VS and Raymer GD: The influence of dominant lethal mutations on litter size and body weight and the consequent impact on transgenerational carcinogenesis. Mutat Res 578: 382-394, 2005.

Biochemical and Biophysical Research Communications 391 (2010) 542–546

Contents lists available at ScienceDirect

Biochemical and Biophysical Research Communications

journal homepage: www.elsevier.com/locate/ybbrc

Roles of POLD4, smallest subunit of DNA polymerase δ, in nuclear structures and genomic stability of human cells

Qin Miao Huang [a], Tomohiro Akashi [b], Yuji Masuda [c], Kenji Kamiya [c], Takashi Takahashi [a], Motoshi Suzuki [a,*]

[a] Division of Molecular Carcinogenesis, Center for Neurological Diseases and Cancer, Nagoya University Graduate School of Medicine, Nagoya, Japan
[b] Division of Molecular Mycology and Medicine, Center for Neurological Diseases and Cancer, Nagoya University Graduate School of Medicine, Nagoya, Japan
[c] Research Institute for Radiation Biology and Medicine, Hiroshima University, Hiroshima 734-8553, Japan

ARTICLE INFO

Article history:
Received 13 November 2009
Available online 24 November 2009

Keywords:
POLD4
Karyomere
Micronuclei
Cell cycle
DNA replication
DNA damage

ABSTRACT

Mammalian DNA polymerase δ (pol δ) is essential for DNA replication, though the functions of this smallest subunit of POLD4 have been elusive. We investigated pol δ activities *in vitro* and found that it was less active in the absence of POLD4, irrespective of the presence of the accessory protein PCNA. shRNA-mediated reduction of POLD4 resulted in a marked decrease in colony formation activity by Calu6, ACC-LC-319, and PC-10 cells. We also found that POLD4 reduction was associated with an increased population of karyomere-like cells, which may be an indication of DNA replication stress and/or DNA damage. The karyomere-like cells retained an ability to progress through the cell cycle, suggesting that POLD4 reduction induces modest genomic instability, while allowing cells to grow until DNA damage reaches an intolerant level. Our results indicate that POLD4 is required for the *in vitro* pol δ activity, and that it functions in cell proliferation and maintenance of genomic stability of human cells.

Introduction

Eukaryotic DNA polymerase δ (pol δ), a key enzyme that participates in DNA replication and repair, consists of four subunits; POLD1 (catalytic subunit, alternatively called p125), POLD2 (p50), POLD3 (p68), and POLD4 (p12) [1,2]. Among those, POLD4 binds to POLD1, POLD2, and an accessory protein of PCNA, which allows pol δ to exhibit its full activity [1,3].

A previous study showed that the *POLD4* ortholog of *Cdm1* in *Schizosaccharomyces pombe* is a non-essential gene related to cell growth, division, and sensitivity to DNA damaging reagents [4]. *Saccharomyces cerevisiae* does not have a POLD4 counterpart, indicating that POLD4 is dispensable in lower eukaryotic cells. In contrast, siRNA-mediated knockdown of POLD4 caused a significant decrease in the proliferation rate of FGF2-activated mouse-endothelial cells [5]. However, it remains unknown whether POLD4 is required for other types of mammalian cells, such as those related to human cancer, or if it has additional functions in mammalian cells.

In the present study, we analyzed the roles of POLD4 for cell proliferation in human lung cancer cell lines. Our findings indicate that POLD4 is required for maintaining the proper nuclear structures and suggest that the pathological structures reflect elevated DNA damage in chromosomes.

Materials and methods

Antibodies. The antibodies used in this study were anti-POLD4 (POLD4 subunit of pol δ) ascites (2B11, Abnova, Taipei City, Taiwan), anti-lamin B (c-20) (Santa Cruz Biotechnology, Santa Cruz, CA), and anti-γ-tubulin (Sigma–Aldrich, St. Louis, MO).

In vitro pol δ activity. Three- and 4-subunit DNA from pol δ were expressed in *Escherichia coli*, and purified as described previously [6]. pol δ activity was determined in a reaction mixture (25 μl) containing 20 mM HEPES–NaOH (pH 7.5), 50 mM NaCl, 0.2 mg/ml BSA, 1 mM dithiothreitol, 10 mM $MgCl_2$, 1 mM ATP, 0.1 mM each of dGTP, dATP, dCTP, and [α-^{32}P]dTTP, 100 ng poly dA-oligo dT (GE Healthcare, Piscataway, NJ), 86 ng (1.0 pmol as a trimer) of PCNA, and 11–88 ng (46–372 fmol) of pol δ at 30 °C for 10 min. Following incubation, the reactions were terminated with 2 μl of 300 mM EDTA. pol activity was determined with reference to the incorporation of [α-^{32}P]dTMP, as previously described [6].

Colony formation assay. To assess cell proliferation, colony formation assays were performed as previously described [7]. In order to rule out the off-target effect, we designed two independent DNA sequences as follows: MS543F, 5′-GATCCCCagtctctggcatctctatcATTCAAGAGATgatagagatgccagagactTTTTTGGAAA-3; MS544R, 5′-AGCTTTTCCAAAAAagtctctggcatctctatcATCTCTTGAATgatagagatgccagagactGGG-3; MS551F, 5′-GATCCCCgcatctctatcccctatgaATTCAAGAGATtcataggggatagagatgcTTTTTGGAAA-3; and MS552R, 5′-AGCTTTTCCAAAAAgcatctctatcccctatgaATCTCTTGAATtcataggggatagagatgcGGG-3, in which the targeting sequences are indicated in lowercase letters. To construct shRNA vectors, MS543F and MS544R

* Corresponding author. Address: Division of Molecular Carcinogenesis, Center for Neurological Diseases and Cancer, Nagoya University Graduate School of Medicine, Nagoya 466-8550, Japan.
E-mail address: msuzuki@med.nagoya-u.ac.jp (M. Suzuki).

0006-291X/$ - see front matter © 2009 Elsevier Inc. All rights reserved.
doi:10.1016/j.bbrc.2009.11.094

(polD4-5), and MS551F and MS552R (polD4-3-1) were annealed, then inserted between the restriction sites BglII and HindIII in PH1RNAneo [7]. Cells transfected with a vector carrying either polD4-3-1 or polD4-5 were cultured in media containing 1 mg/ml G418 (Invitrogen, Carlsbad, CA 10131-027), which was reduced by 0.2 mg/ml every 2 days until it reached 0.4 mg/ml. When colonies grew to visible seizes, they were fixed by cold methanol for 5 min and stained with 4% Giemsa for 15 min at room temperature.

RNA interference. Transfection was carried out using 50 nmol/L of a small interfering RNA (siRNA) duplex (Sigma–Aldrich) targeting each mRNA, or negative control 1# (Ambion) with Lipofectamine-2000 (Invitrogen). The sequences of si*POLD4* were the same as those of polD4-3-1: *POLD4* (si*D4*) sense, 5′-GCAUCUCUAUCCCCUAUGATT-3′; and antisense, 5′-UCAUAGGGGAUAGAGAUGCTT.

Laser scanning cytometry (LSC). Following an overnight culture, 3×10^5/ml Calu6 cells on coverslips were fixed by cold methanol, washed with PBS, and incubated with 1 mg/ml RNase A in 50 mM Tris–HCl, pH 7.5, at 37 °C for 1 h. Cells were further treated with 50 μg/ml propidium iodide in a mixture containing 180 mM Tris–HCl, pH 7.5, 180 mM NaCl, and 70 mM $MgCl_2$ for 15 min. Nuclei structures and DNA contents were analyzed using a Laser Scanning Cytometer (LSC, Olympus, Tokyo, Japan), with DNA content at the G1 peak regarded as 2N, though Calu6 cells carry a greater amount of DNA chromatin than normal cells.

Cell cycle synchronization. Calu6 cells were synchronized according to the method of Nakagawa et al. [8], with minor modifications. In brief, 24-h treatment with 2 mM thymidine was used to arrest exponentially proliferating cells in the S phase. Cells were then released from arrest by three washes in PBS and grown in fresh medium for 15 h, then 1 μM of aphidicolin was used for the second block for 10 h. After releasing by three washes in PBS, cells were incubated in RPMI1640 containing 5% fetal bovine serum and harvested at various time points.

Immunofluorescence. Following an overnight culture, 3×10^5/ml Calu6 cells on coverslips were transfected with siRNA as described above. After 48 h, they were fixed in 4% paraformaldehyde for 10 min at room temperature, followed by treatment with cold methanol for 2 min. The coverslips were washed three times in PBS, treated with PBS containing 0.25% Triton X-100 on ice for 30 min, and incubated with anti-lamin B or anti-γ-tubulin antibody overnight at 4 °C. The cells were then washed three times in PBS, incubated for 1 h with Alexa 488-conjugated secondary antibody (Molecular Probes, OR, USA), and analyzed using an Olympus BX60 (Olympus).

Results and discussion

DNA synthesis activities of pol δ with or without POLD4 in vitro

In order to analyze POLD4 functions related to intrinsic pol δ activity, 3- and 4-subunit structures of pol δ were expressed and purified. In the absence of POLD4, pol δ was less active than the holoenzyme in a reaction containing poly dA–dT as a template primer (Fig. 1A), with a similar result obtained when the accessory protein of PCNA was omitted from the reaction (Fig. 1B). These results are consistent with those of previous studies [1,3] and indicate that POLD4 is required for pol δ to exhibit its full catalytic activity.

POLD4 required for cell proliferation

A previous genetic study of *S. pombe* demonstrated that the *POLD4* ortholog of *Cdm1* is a non-essential gene for cell growth,

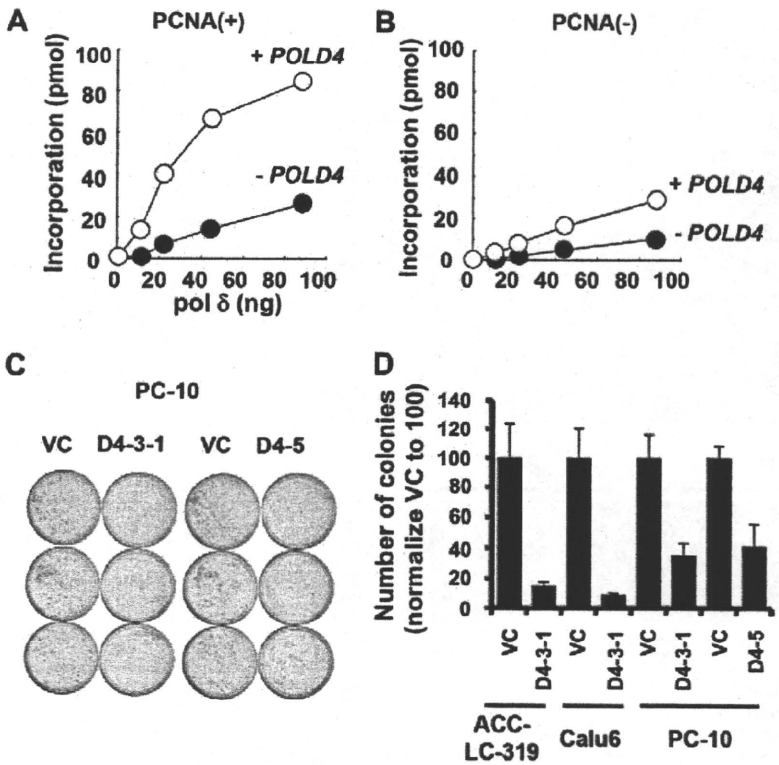

Fig. 1. *In vitro* DNA synthesis activities of pol δ and effect of POLD4 depletion on colony formation activity. (A) pol δ activities were measured and plotted as described in Materials and methods. (B) The same reactions were carried out in the absence of PCNA. (C) PC-10 was used for transfection with plasmids carrying either D4-3-1 or D4-5, and colony formation activity was determined as described in Materials and methods. VC represents vector control. (D) Results of the colony formation assay were plotted in a graph.

division, and sensitivity to DNA damaging reagents [4]. Nevertheless, it is possible that mammalian cells with larger genomic sizes require POLD4 for efficient and accurate DNA replication. We investigated this possibility using shRNA-mediated knockdown of *POLD4*. As shown in Fig. 1C, two independent sequences of shRNA caused reduced activity in a colony formation assay using PC-10, a human non-small cell lung cancer (NSCLC) cell line. Similar results were obtained with different NSCLC cell lines, Calu6 and ACC-LC-319 (Fig. 1D). These findings suggest that human cells require POLD4 for proliferation.

Structure and population of karyomere-like cells following siPOLD4 treatment

Since pol δ is a major DNA replication and repair polymerase, impairment of its activity may cause DNA replication stress, such as accumulation of single-stranded DNA gaps, and inefficient repair of endogenous DNA damage, which ultimately results in cell death. On the other hand, it is also possible that some cells continue to grow following such genetic erosion, which may cause genomic instability. Therefore, we investigated whether POLD4 is also required for suppressing genomic instability in human cells. Initially, we attempted to establish stable clones with low POLD4 expression using shRNA-treated cells. However, clones with adequate levels of POLD4 expression were gradually selected, leading to recovery to the original level over time (data not shown). Therefore, in the following experiments, we used siRNA to transiently reduce POLD4 expression (Fig. 2A, left).

Calu6 cells treated with si*POLD4* formed multiple or lobed nuclei, at a 5.3-fold greater frequency than in the control experiment (Fig. 2B and C). Similar structures were also observed when A549 cells were treated with si*POLD4* (data not shown). Staining with

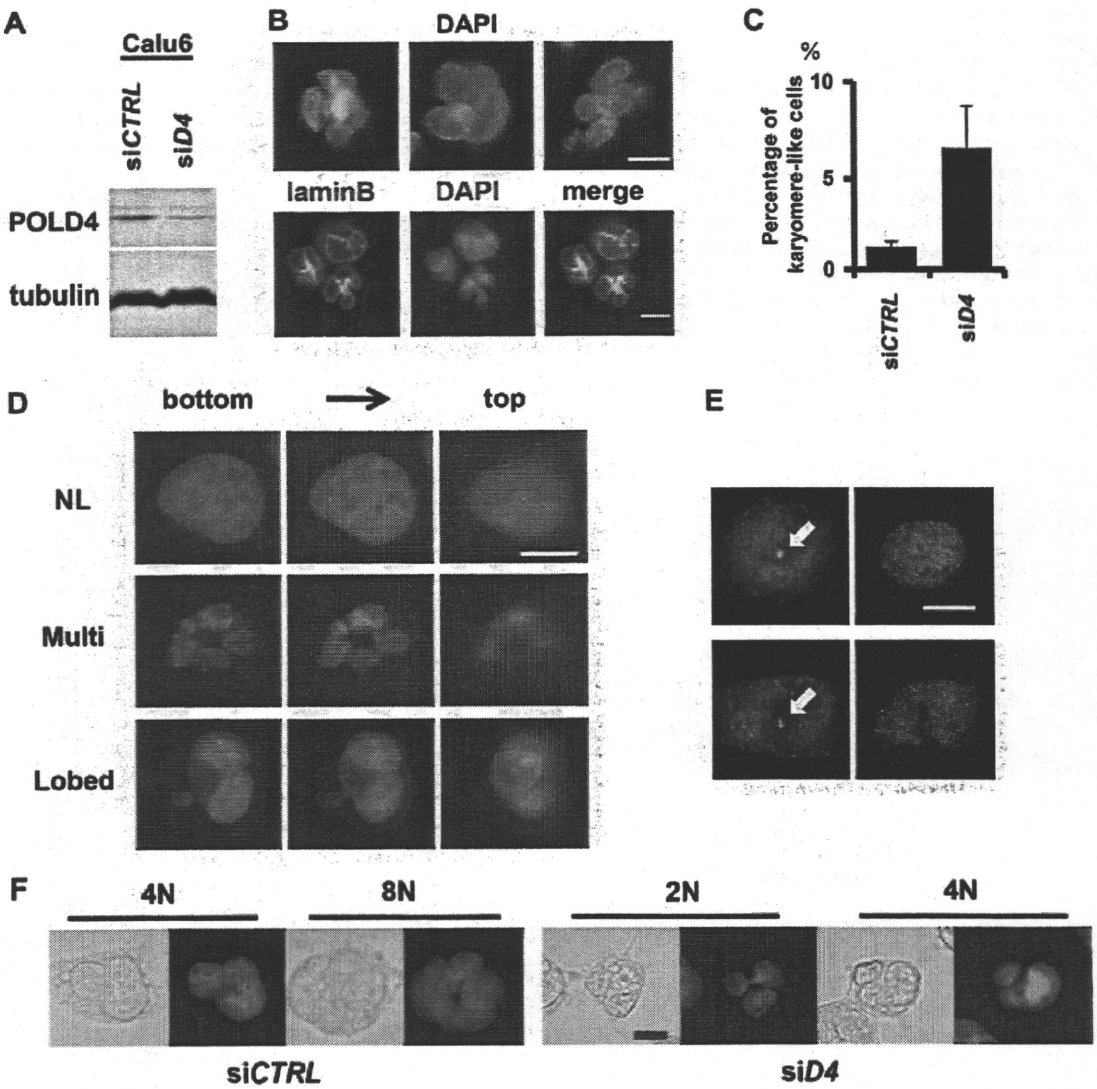

Fig. 2. Structures and population of karyomere-like cells upon si*POLD4* treatment. (A) Western blot analysis of POLD4 and α-tubulin in protein extracts from si*POLD4*- or si*CTRL*-treated Calu6 cells. (B) Upper panels: Calu6 cells were treated with si*POLD4* for 48 h and stained with DAPI. Sample karyomere-like nuclei are shown. Lower panels: Calu6 cells were treated with si*POLD4* for 48 h, then visualized with anti-lamin B antibody or DAPI. (C) Calu6 cells were treated with si*POLD4* or si*CTRL*, then the frequencies of karyomere-like structures in 1000 cells were counted and plotted. In this experiment, cells with three or more nuclear lobes, or three or more nuclei were regarded as karyomere-like cells. Averages of three independent results are shown with SD. (D) si*POLD4*-treated cells were stained by DAPI, then three sequential photographs were taken every 4 μm from the bottom. Upper, middle, and lower panels show images of normal, multiple, and lobed nuclear structures, respectively. (E) After being treated with si*POLD4*, cells were visualized with anti-γ-tubulin (left) or DAPI (right). Upper and lower panels show representative pictures of normal and karyomere-like nuclei, respectively. Centrosomes are indicated by arrows. (F) LSC analysis. Phase-contrast and propidium iodide-stained images of karyomere-like cells among 4N and 8N (si*CTRL*), or 2N and 4N (si*POLD4*) cells. Bar indicates 10 μm.

the anti-lamin B antibody outlined the edges of the DAPI structures and showed that the nuclear envelope was formed around chromatin (Fig. 2B, lower). Sequential acquisition of images from the bottom of the cells further illustrated the abnormal structures of single cells, including a flat profile and multiple nuclei (Fig. 2D, middle panels), or a single nucleus associated with multiple lobes (Fig. 2D, lower panels). For both types of abnormal structures, the nuclear sizes were approximately that of a normally shaped nucleus (Fig. 2D, upper panels).

The multiple nuclei seen with these structures were reminiscent of 'micronuclei' that indicated the presence of DNA damage and DNA replication stress in previous studies [9–11], while the lobed nuclei closely resembled 'karyomere' nuclei observed in zebrafish blastomeres [12] and early *Xenopus laevis* development [13]. In that latter study and other studies referenced therein, it was suggested that karyomere formation is a physiological mitotic process that may share similar mechanisms with pathological micronuclei formation; with both multiple and lobed nuclei, isolated chromosomes might

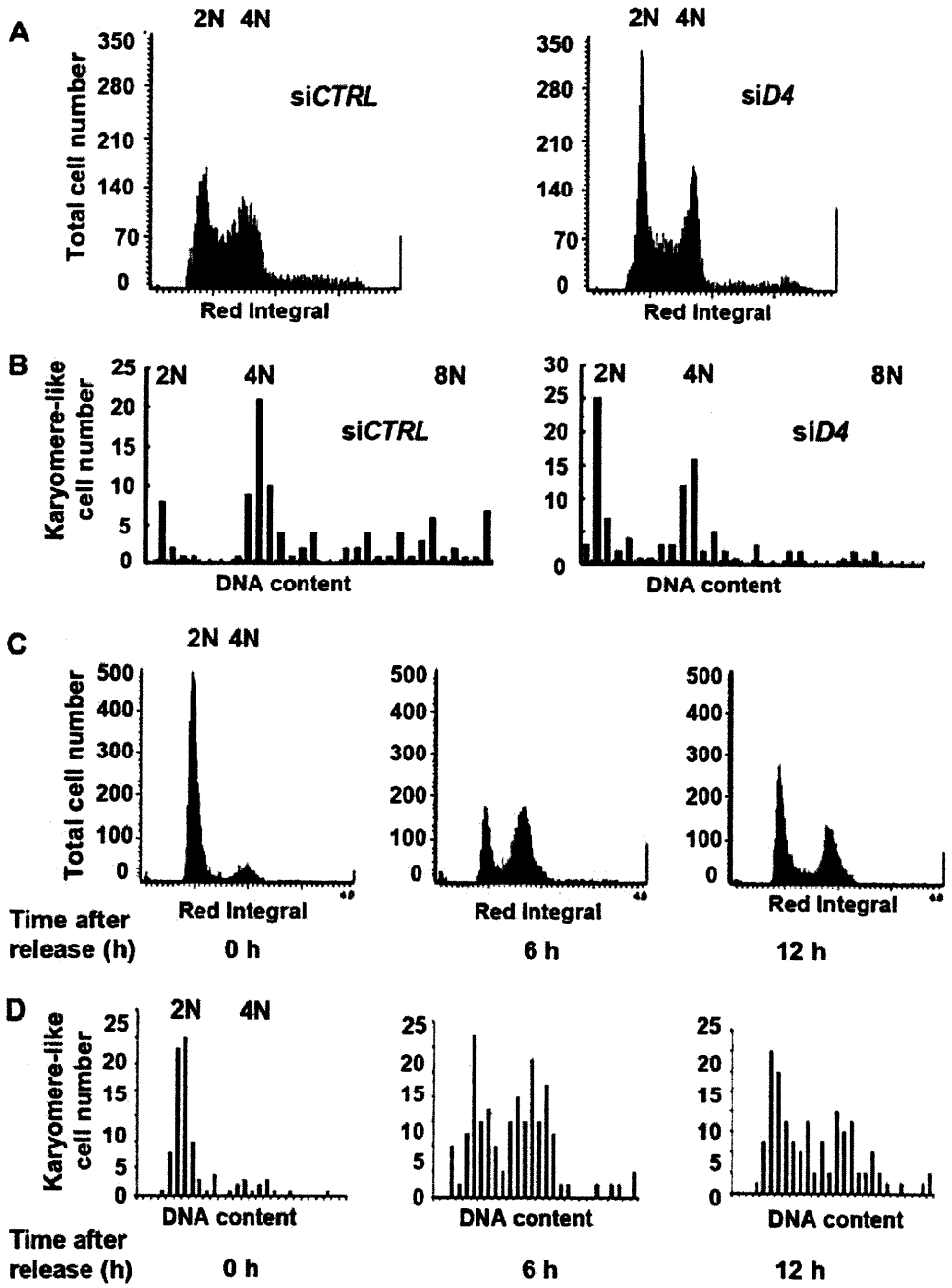

Fig. 3. Cell cycle dynamics of karyomere-like cells. (A) Calu6 cells were treated with si*CTRL* (left) or si*POLD4* (right), then their DNA contents were subjected to LSC analysis. The G1 population found among the majority of cells was regarded as 2N. (B) In the same experiment, DNA contents of 100 karyomere-like cells were determined. Cell numbers in each DNA content range were plotted with histograms. (C) Calu6 cells were treated with si*POLD4*, then synchronized at the G1/S boundary and released for cell cycle progression. At 0, 6, or 12 h after release, DNA contents were subjected to LSC. (D) In the same experiment, the DNA contents of 100 karyomere-like cells were measured. Cell numbers in each DNA content range were plotted with histograms.

be surrounded by a nuclear envelope after chromosome segregation occurs. Therefore, those two types of abnormal structures are referred to as karyomere-like nuclei hereafter.

In addition to DNA damage, formation of karyomere-like nuclei may also occur as a consequence of dysfunctions of the mitotic apparatus [13,14]. Moreover, a previous study found that the anti-POLD4 antibody bound the surface of mitotic chromosomes, which suggests specific functions of POLD4 during mitosis [5]. To investigate this, we analyzed the centrosome structures in si *POLD4*-treated cells, as it has been reported that disturbed chromosomal migration occurred with abnormal replication or localization of centrosomes [15,16]. Our present results showed that si *POLD4*-treated cells were associated with normal centrosome structures, which had one or two centrosomes located at a single site (Fig. 2E). We also quantified the lagging-chromosome frequencies, and found that they were very similar between si*POLD4*- and si*CTRL*-treated mitotic cells (data not shown). Although the results of this limited experiment were contrary to our speculation that POLD4 has some mitotic functions, we intend to conduct more detailed examinations in the future.

Cell cycle dynamics of karyomere-like cells

In the following experiments, we studied the cell cycle dynamics of karyomere-like cells. After si*POLD4* treatment, we observed checkpoint activation (data not shown, detailed mechanisms discussed elsewhere), and accumulations of G1- and G2-populations (Fig. 3A). In si*CTRL*-treated cells, most of the karyomere-like populations were found among the minor aneuploid populations (Figs. 3B and 2F, left panels). In contrast, karyomere-like cells in si *POLD4*-treated cells were found to have normal ploidy as seen with 2N–4N cells (Fig. 3B, 2F, right panels).

In order to determine if karyomere-like cells remained alive and had an ability to progress through the cell cycle, we synchronized cells at the G1–S boundary, then released them and observed the cell cycle progression, as well as the associated nuclear shapes (Fig. 3C–E). Interestingly, karyomere-like cells progressed through the cell cycle and returned to G1 at 12 h after release. In support of these results, most karyomere-like cells were negative in TUNEL staining findings (data not shown). Therefore, these structures may not reflect the pro-apoptotic phenotype. Our results suggest that most karyomere-like cells are able to proliferate until they became arrested at the G1 or G2 phase, when DNA damage reaches an intolerant level.

In conclusion, our results showed that POLD4 supports cellular proliferation and suppresses karyomere-like nuclei formation in human cells, which might occur as a consequence of impairment of the DNA replication and repair activities of pol δ. A future study to identify the direct link between POLD4 and mitotic functions may reveal the underlying mechanisms to maintain genomic stability in human cells.

Acknowledgments

We thank Keiko Ueda and Makiko Terada for their initial involvement in this project. We are also grateful for Dr. Takeshi Senga of our university for the critical reading of the manuscript. This work was supported in part by a Grant-in-Aid for Scientific Research on Innovative Areas, a Grant-in-Aid for Scientific Research on Priority Areas from the Ministry of Education, Culture, Sports, Science, and Technology of Japan, and a Grant-in-Aid for Scientific Research from the Japan Society for the Promotion of Science.

References

[1] V.N. Podust, L.S. Chang, R. Ott, G.L. Dianov, E. Fanning, Reconstitution of human DNA polymerase delta using recombinant baculoviruses: the p12 subunit potentiates DNA polymerizing activity of the four-subunit enzyme, J. Biol. Chem. 277 (2002) 3894–3901.
[2] L. Liu, J. Mo, E.M. Rodriguez-Belmonte, M.Y. Lee, Identification of a fourth subunit of mammalian DNA polymerase delta, J. Biol. Chem. 275 (2000) 18739–18744.
[3] H. Li, B. Xie, Y. Zhou, A. Rahmeh, S. Trusa, S. Zhang, Y. Gao, E.Y. Lee, M.Y. Lee, Functional roles of p12, the fourth subunit of human DNA polymerase delta, J. Biol. Chem. 281 (2006) 14748–14755.
[4] N. Reynolds, A. Watt, P.A. Fantes, S.A. MacNeill, Cdm1, the smallest subunit of DNA polymerase d in the fission yeast *Schizosaccharomyces pombe*, is non-essential for growth and division, Curr. Genet. 34 (1998) 250–258.
[5] P. Dell'Era, S. Nicoli, G. Peri, M. Nieddu, M.G. Ennas, M. Presta, FGF2-induced upregulation of DNA polymerase-delta p12 subunit in endothelial cells, Oncogene 24 (2005) 1117–1121.
[6] Y. Masuda, M. Suzuki, J. Piao, Y. Gu, T. Tsurimoto, K. Kamiya, Dynamics of human replication factors in the elongation phase of DNA replication, Nucleic Acids Res. 35 (2007) 6904–6916.
[7] H. Tanaka, K. Yanagisawa, K. Shinjo, A. Taguchi, K. Maeno, S. Tomida, Y. Shimada, H. Osada, T. Kosaka, H. Matsubara, T. Mitsudomi, Y. Sekido, M. Tanimoto, Y. Yatabe, T. Takahashi, Lineage-specific dependency of lung adenocarcinomas on the lung development regulator TTF-1, Cancer Res. 67 (2007) 6007–6011.
[8] T. Nakagawa, Y. Hayashita, K. Maeno, A. Masuda, N. Sugito, H. Osada, K. Yanagisawa, H. Ebi, K. Shimokata, T. Takahashi, Identification of decatenation G2 checkpoint impairment independently of DNA damage G2 checkpoint in human lung cancer cell lines, Cancer Res. 64 (2004) 4826–4832.
[9] N. Holland, C. Bolognesi, M. Kirsch-Volders, S. Bonassi, E. Zeiger, S. Knasmueller, M. Fenech, The micronucleus assay in human buccal cells as a tool for biomonitoring DNA damage: the HUMN project perspective on current status and knowledge gaps, Mutat. Res. 659 (2008) 93–108.
[10] J.B. Bae, S.S. Mukhopadhyay, L. Liu, N. Zhang, J. Tan, S. Akhter, X. Liu, X. Shen, L. Li, R.J. Legerski, Snm1B/Apollo mediates replication fork collapse and S phase checkpoint activation in response to DNA interstrand cross-links, Oncogene 27 (2008) 5045–5056.
[11] D.J. Kirkland, L. Henderson, D. Marzin, L. Muller, J.M. Parry, G. Speit, D.J. Tweats, G.M. Williams, Testing strategies in mutagenicity and genetic toxicology: an appraisal of the guidelines of the European Scientific Committee for Cosmetics and Non-Food Products for the evaluation of hair dyes, Mutat. Res. 588 (2005) 88–105.
[12] V.K. Schoft, A.J. Beauvais, C. Lang, A. Gajewski, K. Prufert, C. Winkler, M.A. Akimenko, M. Paulin-Levasseur, G. Krohne, The lamina-associated polypeptide 2 (LAP2) isoforms beta, gamma and omega of zebrafish: developmental expression and behavior during the cell cycle, J. Cell Sci. 116 (2003) 2505–2517.
[13] J.M. Lemaitre, G. Geraud, M. Mechali, Dynamics of the genome during early *Xenopus laevis* development: karyomeres as independent units of replication, J. Cell Biol. 142 (1998) 1159–1166.
[14] M. Ohsugi, K. Adachi, R. Horai, S. Kakuta, K. Sudo, H. Kotaki, N. Tokai-Nishizumi, H. Sagara, Y. Iwakura, T. Yamamoto, Kid-mediated chromosome compaction ensures proper nuclear envelope formation, Cell 132 (2008) 771–782.
[15] D. Eriksson, P.O. Lofroth, L. Johansson, K.A. Riklund, T. Stigbrand, Cell cycle disturbances and mitotic catastrophes in HeLa Hep2 cells following 2.5 to 10 Gy of ionizing radiation, Clin. Cancer Res. 13 (2007) 5501s–5508s.
[16] H. Dodson, E. Bourke, L.J. Jeffers, P. Vagnarelli, E. Sonoda, S. Takeda, W.C. Earnshaw, A. Merdes, C. Morrison, Centrosome amplification induced by DNA damage occurs during a prolonged G2 phase and involves ATM, EMBO J. 23 (2004) 3864–3873.

Published online 17 July 2010

Nucleic Acids Research, 2010, Vol. 38, No. 21 7579–7586
doi:10.1093/nar/gkq630

Single-stranded DNA catenation mediated by human EVL and a type I topoisomerase

Motoki Takaku[1], Daisuke Takahashi[1], Shinichi Machida[1], Hiroyuki Ueno[1], Noriko Hosoya[2], Shukuko Ikawa[3], Kiyoshi Miyagawa[2], Takehiko Shibata[3] and Hitoshi Kurumizaka[1,*]

[1]Laboratory of Structural Biology, Graduate School of Advanced Science and Engineering, Waseda University, 2-2 Wakamatsu-cho, Shinjuku-ku, Tokyo 162-8480, [2]Laboratory of Molecular Radiology, Center of Disease Biology and Integrative Medicine, Graduate School of Medicine, The University of Tokyo, 7-3-1 Hongo, Bunkyo-ku, Tokyo 113-0033 and [3]RIKEN Advanced Science Institute, 2-1 Hirosawa, Wako-shi, Saitama 351-0198, Japan

Received April 5, 2010; Accepted June 30, 2010

ABSTRACT

The human Ena/Vasp-like (EVL) protein is considered to be a bifunctional protein, involved in both actin remodeling and homologous recombination. In the present study, we found that human EVL forms heat-stable multimers of circular single-stranded DNA (ssDNA) molecules in the presence of a type I topoisomerase *in vitro*. An electron microscopic analysis revealed that the heat-stable ssDNA multimers formed by EVL and topoisomerase were ssDNA catemers. The ssDNA catenation did not occur when either EVL or topoisomerase was omitted from the reaction mixture. A deletion analysis revealed that the ssDNA catenation completely depended on the annealing activity of EVL. Human EVL was captured from a human cell extract by TOPO IIIα-conjugated beads, and the interaction between EVL and TOPO IIIα was confirmed by a surface plasmon resonance analysis. Purified TOPO IIIα catalyzed the ssDNA catenation with EVL as efficiently as the *Escherichia coli* topoisomerase I. Since the ssDNA cutting and rejoining reactions, which are the sub-steps of ssDNA catenation, may be an essential process in homologous recombination, EVL and TOPO IIIα may function in the processing of DNA intermediates formed during homologous recombination.

INTRODUCTION

Human Ena/Vasp-like (EVL) is a member of the ENA/VASP family, which is involved in actin-remodeling processes (1). We previously reported (2) that EVL may also function in homologous recombination, because it directly binds to RAD51 and RAD51B, which are essential proteins for meiotic homologous recombination and mitotic recombinational repair of DNA double-strand breaks (3–6). Biochemical studies revealed that EVL forms tetramer-based multimers, and actually stimulates the RAD51-mediated recombinase reactions, such as homologous pairing and strand exchange, *in vitro* (2,7). In addition to the RAD51-stimulating activity, EVL also possesses ssDNA annealing activity (2), which is considered to be important for the homologous-recombination processes. Therefore, EVL may have dual functions in cytoplasmic actin remodeling and nuclear homologous recombination.

Topoisomerases promote DNA strand cutting and rejoining, and are known to be important in homologous recombination. *Escherichia coli* RecA, a bacterial homolog of RAD51, forms homologous joint molecules between circular ssDNA and closed circular dsDNA by its recombinase activity (8). *Escherichia coli* topoisomerase I (Topo I) reportedly converts the homologous joint molecules formed by RecA into hemicatemers (8). *Escherichia coli* topoisomerase III efficiently catenates closed circular dsDNAs in the presence of RecQ helicase (9,10), which is suggested to function in homologous recombination. In humans, TOPO IIIα forms a complex with BLM and BLAP75 (11,12), and the complex is reportedly involved in the dissolution of the Holliday junction (13–18), which is a DNA intermediate formed in the late stage of homologous recombination. These facts suggest that the DNA cutting and rejoining activities of topoisomerases play important roles in homologous recombination.

In the present study, we unexpectedly found that EVL, with either *E. coli* Topo I or human TOPO IIIα, catalyzed

*To whom correspondence should be addressed. Tel: +81 3 5369 7315; Fax: +81 3 5367 2820; Email: kurumizaka@waseda.jp